cyte apoptosis in Bcl-xL- or Mcl-1-knock-out mice (7, 13). In the present study, we focused on another BH3-only protein, Bim, which promotes hepatocyte apoptosis upon activation by free fatty acids or by reactive oxygen species in pathological settings, and we further clarified the orchestration of the Bcl-2 network, which governs hepatocyte life and death in the physiological state (10, 11, 14, 15). We found that the disruption of Bim ameliorated hepatocyte apoptosis in Bcl-xL- or Mcl-1-knock-out mice, indicating the involvement of Bim in this hepatocyte apoptosis machinery in the healthy liver as well as that of Bid. Additionally, the deletion of both Bim and Bid prevented the massive hepatocyte apoptosis caused by the inhibition of both Bcl-xL and Mcl-1, suggesting that Bim and Bid are functionally active in the healthy liver and are essential regulators for promoting the intrinsic pathway of apoptosis in hepatocytes in the absence of anti-apoptotic Bcl-2 family proteins. Our present study unveiled the fine and dynamic Bcl-2 networks, the orchestration of which determines hepatocyte life and death in the healthy liver.

EXPERIMENTAL PROCEDURES

Mice—Mice carrying a *bcl-x* gene with two *loxP* sequences at the promoter region and a second intron (*bcl-x*$^{flox/flox}$), mice carrying an *mcl-1* gene encoding amino acids 1–179 flanked by two *lox*P sequences, and heterozygous *alb-cre* transgenic mice expressing the Cre recombinase gene under regulation of the *albumin* gene promoter have been described previously (16–18). Hepatocyte-specific Bcl-xL-knock-out mice (*bcl-x*$^{flox/flox}$*alb-cre*) (17), hepatocyte-specific Mcl-1-knock-out mice (*bcl-x*$^{flox/flox}$*alb-cre*) (13), systemic Bid-knock-out mice (*bid*$^{-/-}$) (12), and Bcl-xL/Bid double knock-out mice (*bid*$^{-/-}$*bcl-x*$^{flox/flox}$*alb-cre*) (7) have also been described previously. We purchased C57BL/6J mice from Charles River (Osaka, Japan), systemic Bim-knock-out mice (*bim*$^{-/-}$) from the Jackson Laboratory (Bar Harbor, ME), and NOD/ShiJic-*scid* Jcl mice from Clea Japan Inc. (Osaka, Japan). We generated Bcl-xL/Bim double knock-out mice (*bim*$^{-/-}$*bcl-x*$^{flox/flox}$*alb-cre*), Mcl-1/Bim double knock-out mice (*bim*$^{-/-}$*mcl-1*$^{flox/flox}$*alb-cre*), Bcl-xL/Bim/Bid triple knock-out mice (*bim*$^{-/-}$*bid*$^{-/-}$*bcl-x*$^{flox/flox}$*alb-cre*), and Bim/Bid double knock-out mice (*bim*$^{-/-}$*bid*$^{-/-}$) by mating the strains. We generated mice with a hepatocyte-specific deletion of Mcl-1 and homozygote severe combined immune deficiency (SCID) mutations (*mcl-1*$^{flox/flox}$*prkdc*$^{scid/scid}$*alb-cre*) by mating hepatocyte-specific Mcl-1-knock-out mice (*bcl-x*$^{flox/flox}$*alb-cre*) and NOD/ShiJic-*scid* Jcl mice. Genotyping of *prkdc*^{scid} gene mutation was performed by the PCR-confronting two-pair primer (PCR-CTPP) method reported previously (19). The mice were maintained in a specific pathogen-free facility and were afforded humane care under approval from the Animal Care and Use Committee of Osaka University Medical School.

Histological Analyses—Liver sections were stained with hematoxylin and eosin (H&E). To detect apoptotic cells, the liver sections were also subjected to staining by terminal deoxynucleotidyltransferase-mediated deoxyuridine triphosphate nick-end labeling (TUNEL) according to a procedure reported previously (20). For immunohistochemical detection of cleaved caspase-3, the liver sections were incubated with the polyclonal rabbit anti-cleaved caspase-3 antibody (Cell Signaling Technology, Beverly, MA) according to a procedure reported previously (20).

Caspase-3/7 Activity—Serum caspase-3/7 activity was measured by a luminescent substrate assay for caspase-3 and caspase-7 (Caspase-Glo assay, Promega) according to the manufacturer's protocol.

Western Blot Analysis—Liver tissue was lysed in lysis buffer (1% Nonidet P-40, 0.5% sodium deoxycholate, 0.1% SDS, 1× protein inhibitor mixture (Nacalai tesque, Kyoto, Japan), 1× phosphatase inhibitor mixture (Nacalai tesque), and phosphate-buffered saline, pH 7.4). The liver lysates were cleared by centrifugation at 10,000 × *g* for 15 min at 4 °C. The protein concentrations were determined using a bicinchoninic acid protein assay kit (Pierce). The protein lysates were electrophoretically separated with SDS-polyacrylamide gels and were transferred onto a polyvinylidene fluoride membrane. For immunodetection, the following antibodies were used: a rabbit polyclonal antibody to Bcl-xL (Santa Cruz Biotechnology, Inc.), a rabbit polyclonal antibody to Bid, a rabbit polyclonal antibody to Bax, a rabbit polyclonal antibody to cleaved caspase-3, a rabbit polyclonal antibody to cleaved caspase-7, a rabbit polyclonal antibody to Puma (Cell Signaling Technology, Beverly, MA), a rabbit monoclonal antibody to Bad, a rabbit polyclonal antibody to Noxa (Abcam, Cambridge, MA), a rabbit polyclonal antibody to Bak (Millipore, Billerica, MA), a rabbit polyclonal antibody to Bim (Enzo Life Sciences Inc., Farmingdale, NY), a rabbit polyclonal antibody to Mcl-1 (Rockland, Gilbertsville, PA), and a mouse monoclonal antibody to β-actin (Sigma-Aldrich).

Real-time Reverse Transcription Polymerase Chain Reaction (Real-time RT-PCR) for mRNA—Total RNA was extracted from liver tissues using an RNeasy minikit (Qiagen, Valencia, CA), was reverse-transcribed, and was subjected to real-time RT-PCR as described previously (21). The mRNA expression of specific genes was quantified using TaqMan gene expression assays (Applied Biosystems, Foster City, CA) as follows: murine *bcl2l11* (assay ID: Mm00437796_m1), murine *fas* (assay ID: Mm01204974_m1), murine *bik* (assay ID: Mm00476123_m1), murine *hrk* (assay ID: Mm01208086_m1), murine *bmf* (assay ID: Mm00506773_m1), and murine *actb* (assay ID: Mm02619580_g1 or Mm00607939_s). The transcript levels are presented as -fold inductions.

siRNA-mediated in Vivo Knockdown—The hepatocyte-specific Bcl-xL-knock-out mice (*bcl-x*$^{flox/flox}$*alb-cre*) and the Bcl-xL/Bim/Bid triple knock-out mice (*bim*$^{-/-}$*bid*$^{-/-}$*bcl-x*$^{flox/flox}$*alb-cre*) were injected with 5 mg/kg *in vivo* grade siRNA against *mcl-1* (MSS275671_e0N), which was mixed with Invivofectamine (Invitrogen), via the tail vein according to the manufacturer's protocol. The mice were sacrificed and examined as indicated by the time courses. The Stealth RNAi negative control with low GC content (Invitrogen) was used as the control.

In Vivo ABT-737 Experiment—ABT-737 was dissolved in a mixture of 30% propylene glycol, 5% Tween 80, and 65% D5W (5% dextrose in water) with pH 4–5. ABT-737 (100 mg/kg) was intraperitoneally administered to the Bim/Bid double knock-

out mice ($bim^{-/-}bid^{-/-}$) or to the Bid-knock-out mice ($bid^{-/-}$). The mice were sacrificed and examined 6 h later.

Statistical Analysis—All of the data are expressed as means ± S.D. unless otherwise indicated. Statistical analyses were performed using an unpaired Student's *t* test or a one-way analysis of variance unless otherwise indicated. When the analyses of variance were applied, the differences in the mean values among the groups were examined by Scheffe's post hoc correction unless otherwise indicated. $p < 0.05$ was considered statistically significant.

RESULTS

The Disruption of Bim Alleviated Spontaneous Hepatocyte Apoptosis in Hepatocyte-specific Bcl-xL-knock-out Mice—To investigate the involvement of the BH3-only protein Bim in the hepatocyte apoptosis caused by Bcl-xL deficiency, hepatocyte-specific Bcl-xL-knock-out mice ($bcl\text{-}x^{fl/fl}alb\text{-}cre$) were mated with systemic Bim-knock-out mice ($bim^{-/-}$). Offspring from the mating of $bim^{+/-}bcl\text{-}x^{fl/fl}alb\text{-}cre$ mice and $bim^{+/-}bcl\text{-}x^{fl/fl}$ mice were examined at 6 weeks of age. A Western blot study confirmed the disappearance of both Bcl-xL and Bim protein expression in the liver tissue of the double knock-out mice ($bim^{-/-}bcl\text{-}x^{fl/fl}alb\text{-}cre$) (Fig. 1*A*). In agreement with our previous report (7, 17), H&E staining of the liver sections showed an increase in the number of hepatocytes, with chromatin condensation and cytosolic shrinkage in the liver lobules of the Bcl-xL-knock-out mice (Fig. 1*B*). The staining also showed a significant increase in TUNEL-positive cells and cleaved caspase-3-positive cells in the liver (Fig. 1, *B–D*). Consistent with these histological observations, the levels of serum caspase-3/7 activity and serum alanine aminotransferase (ALT), which can be used as indicators of hepatocyte apoptosis (22, 23), were significantly higher in the Bcl-xL-knock-out mice than in their wild-type littermates (Fig. 1, *E* and *F*). Additionally, cleaved caspse-3 and -7 were detected in the livers of the Bcl-xL-knock-out mice by Western blotting (Fig. 1*A*). All of these findings indicated spontaneous hepatocyte apoptosis in these mice. Bim-knock-out mice did not show any phenotypes in the liver under physiological conditions (Fig. 1, *B–F*). Alternatively, the disruption of Bim significantly improved all of the parameters that are indicative of hepatocyte apoptosis in Bcl-xL-knock-out mice, including the TUNEL-positive cell counts, cleaved caspase-3-positive cell counts, serum ALT levels, and serum caspase-3/7 activity (Fig. 1, *B–F*). These findings clearly demonstrated that Bim was involved in the hepatocyte apoptosis caused by Bcl-xL disruption. It should be noted that the gene and protein expression levels of Bim were not different between the Bcl-xL-knock-out mice and their wild-type littermates (Fig. 1, *A* and *G*), indicating that the Bim expression levels observed in the healthy liver could induce hepatocyte apoptosis in the absence of the Bcl-2 family proteins.

The Disruption of Bim Alleviated Spontaneous Hepatocyte Apoptosis in Hepatocyte-specific Mcl-1-knock-out Mice—Of the five members of the anti-apoptotic Bcl-2 family proteins, we previously reported that Mcl-1 and Bcl-xL played a pivotal anti-apoptotic role in maintaining hepatocyte integrity in the healthy liver (13). We thus examined the role of Bim in the hepatocyte apoptosis caused by Mcl-1 deficiency. We generated Mcl-1/Bim double knock-out mice ($bim^{-/-}mcl\text{-}1^{fl/fl}alb\text{-}cre$) by mating the hepatocyte-specific Mcl-1-knock-out mice ($mcl\text{-}1^{fl/fl}alb\text{-}cre$) with the systemic Bim-knock-out mice ($bim^{-/-}$). A Western blot study confirmed the disappearance of both Mcl-1 and Bim protein expression in the liver tissue of the double knock-out mice ($bim^{-/-}mcl\text{-}1^{fl/fl}alb\text{-}cre$) (Fig. 2*A*). Consistent with our previous report (13), hepatocyte-specific Mcl-1-knock-out mice showed apoptosis phenotypes very similar to those of the Bcl-xL-knock-out mice, as assessed by TUNEL staining (Fig. 2, *B* and *C*), cleaved caspase-3 staining (Fig. 2, *B* and *D*), serum caspase-3/7 activity (Fig. 2*E*), and serum ALT levels (Fig. 2*F*). In contrast, Mcl-1/Bim double knock-out mice showed significant improvement in these parameters (Fig. 2, *B–F*), indicating that Bim is also involved in the hepatocyte apoptosis induced by the disruption of Mcl-1.

The Disruption of Bim and Bid Prevented Spontaneous Hepatocyte Apoptosis in Hepatocyte-specific Bcl-xL-knock-out Mice—We previously reported that a small amount of Bid, which is another BH3-only protein, was constitutively active and was involved in the spontaneous hepatocyte apoptosis in Bcl-xL- or Mcl-1-knock-out mice (7, 13). We thus examined whether these BH3-only proteins redundantly or cooperatively promoted hepatocyte apoptosis in the absence of Bcl-xL. To this end, Bim/Bid/Bcl-xL triple knock-out mice ($bim^{-/-}bid^{-/-}bcl\text{-}x^{fl/fl}alb\text{-}cre$) were generated by mating the Bim/Bcl-xL double knock-out mice ($bim^{-/-}bcl\text{-}x^{fl/fl}alb\text{-}cre$) with the Bid/Bcl-xL double knock-out mice ($bid^{-/-}bcl\text{-}x^{fl/fl}alb\text{-}cre$). The offspring from the mating of $bim^{+/-}bid{-}/{-}bcl\text{-}x^{fl/fl}alb\text{-}cre$ mice with $bim^{+/-}bid^{-/-}bcl\text{-}x^{fl/fl}$ mice were examined at 6 weeks of age. A Western blot study confirmed that Bcl-xL, Bid, and Bim protein expression disappeared from the liver tissue of the triple knock-out mice ($bim^{-/-}bid^{-/-}bcl\text{-}x^{fl/fl}alb\text{-}cre$) (Fig. 3*A*). Liver sections of the Bim/Bid/Bcl-xL triple knock-out mice were histologically normal compared with those of the Bid/Bcl-xL double knock-out mice ($bim^{+/+}bid^{-/-}bcl\text{-}x^{fl/fl}alb\text{-}cre$), which still contained some hepatocytes with apoptotic morphologies (Fig. 3*B*). Both the number of TUNEL-positive cells and the serum caspase-3/7 activity in the triple knock-out mice were significantly lower than those in the Bid/Bcl-xL double knock-out mice and did not differ from their control Bid-knock-out or Bim/Bid double knock-out littermates (Fig. 3, *B–D*). Moreover, in contrast to the mild elevation of serum ALT levels in the Bid/Bcl-xL double knock-out mice, the levels in the triple knock-out mice were completely normal (Fig. 3*E*). These findings demonstrated that hepatocyte apoptosis in the absence of Bcl-xL was completely dependent on these two BH3-only proteins.

Bim and Bid Are Essential Regulators for the Promotion of the Intrinsic Pathway of Apoptosis in Hepatocytes in the Absence of Anti-apoptotic Bcl-2 Family Proteins—We then attempted to further examine the involvement of Bim and Bid in hepatocyte apoptosis in the absence of both Bcl-xL and Mcl-1, which are two major anti-apoptotic proteins in the liver. Because, as we reported (13), the hepatocyte-specific Bcl-xL and Mcl-1 double knock-out mice died within 1 day after birth due to impaired liver development, we performed an siRNA-mediated *in vivo* knockdown of *mcl-1* in the Bcl-xL-knock-out mice and in the Bim/Bid/Bcl-xL triple knock-out mice. *mcl-1* siRNA administration efficiently reduced Mcl-1 protein expression in the liver

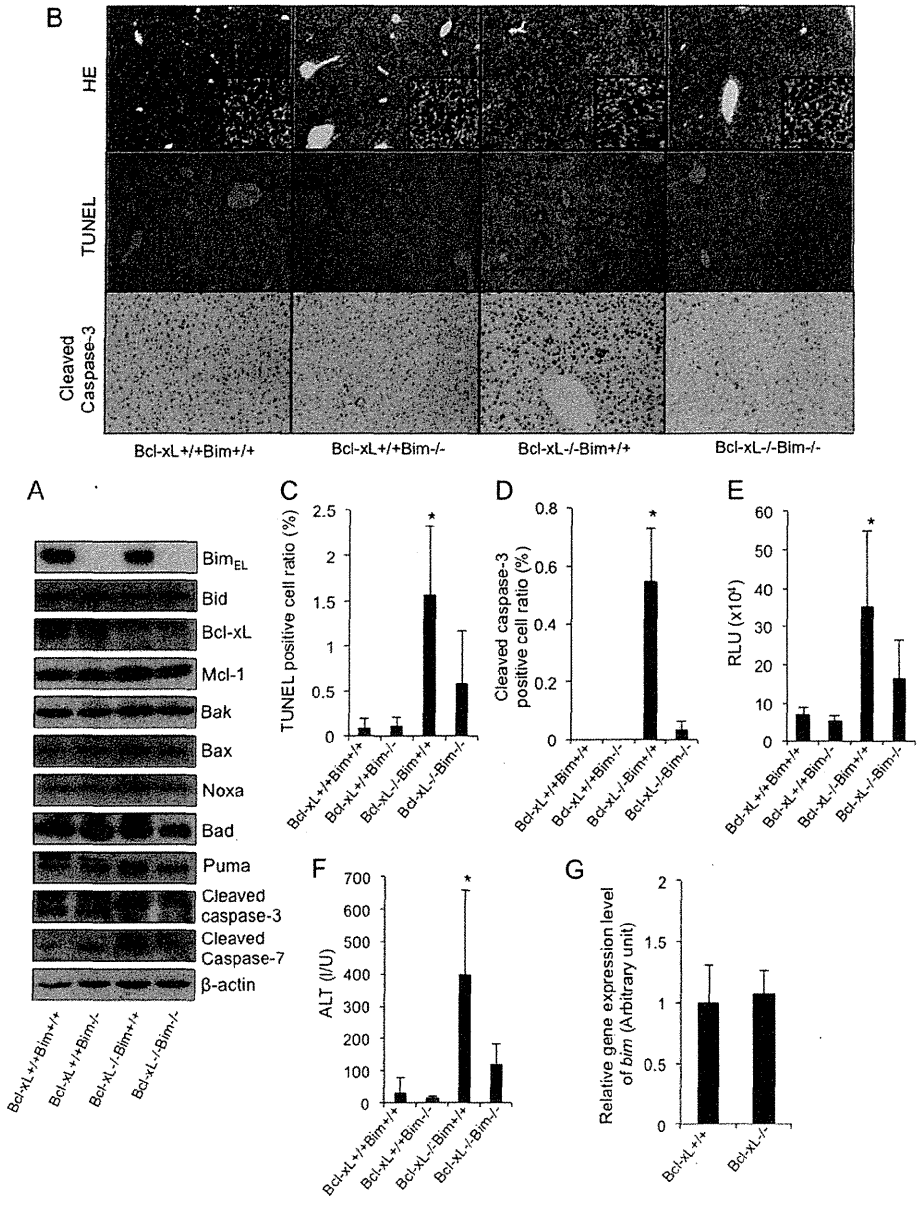

FIGURE 1. **The disruption of Bim alleviated spontaneous hepatocyte apoptosis in the absence of Bcl-xL.** *A–F*, the offspring from the mating of *bim*±*bcl-x*$^{flox/flox}$*alb-cre* mice with *bim*±*bcl-x*$^{flox/flox}$ mice were examined at 6 weeks of age. *Bcl-xL*$^{+/+}$ and *Bcl-xL*$^{-/-}$, *bcl-x*$^{flox/flox}$ and *bcl-x*$^{flox/flox}$*alb-cre*, respectively. *A*, Western blot analysis of whole liver lysates for the expression of Bim$_{EL}$, Bid, Bcl-xL, Mcl-1, Bak, Bax, Noxa, Bad, Puma, cleaved caspase-3, cleaved caspase-7, and β-actin. *B*, representative images for liver histology stained with hematoxylin-eosin (*HE*), TUNEL, and cleaved caspase-3 (original magnifications, ×100 (*large panels*) and ×400 (*insets*)); *black arrows* indicate apoptotic bodies. *C*, TUNEL-positive cell ratio; $n = 8$ mice/group; *, $p < 0.05$ *versus* all. *D*, cleaved caspase-3-positive cell ratio; $n = 3$ mice/group; *, $p < 0.05$ *versus* all. *E*, serum caspase-3/7 activity; $n = 11$ mice/group; *, $p < 0.05$ *versus* all. *F*, serum ALT levels; $n = 13$ mice/group; *, $p < 0.05$ *versus* all. *G*, offspring from the mating of *bcl-x*$^{flox/flox}$*alb-cre* mice with *bcl-x*$^{flox/flox}$ mice were examined at 6 weeks of age. *Bcl-xL*$^{+/+}$ and *Bcl-xL*$^{-/-}$, *bcl-x*$^{flox/flox}$ and *bcl-x*$^{flox/flox}$*alb-cre*, respectively. *bim* mRNA levels in the whole liver tissue were determined by real-time RT-PCR; $n = 6$ mice/group. *Error bars*, S.D. *RLU*, relative light units; *I/U*, international units.

tissue of both mice (Fig. 4*A*), but it caused severe liver injury only in the Bcl-xL-knock-out mice (Fig. 4*B*) when assessed by the H&E staining of liver sections. Notably, *mcl-1* siRNA administration caused massive hepatocyte apoptosis in the Bcl-xL-knock-out mice, but this apoptosis was weakened in the Bim/Bid/Bcl-xL triple knock-out mice, as evidenced by the TUNEL staining of the liver sections, serum caspase-3/7 activity, and serum ALT levels (Fig. 4, *C–E*). In agreement with these findings, *mcl-1* siRNA treatment impaired the liver function of the Bcl-xL-knock-out mice, as evidenced by an increase in the serum bilirubin levels, but not the liver function of the triple knock-out mice (Fig. 4*F*). These findings demonstrated that the massive hepatocyte apoptosis and liver failure caused by decreases in these anti-apoptotic Bcl-2 family proteins were dependent on Bid and Bim.

The Presence of Bim- and Bid-induced Constant BH3 Stress in the Healthy Liver Causes Hepatotoxicity with the Use of Anti-cancer Agents That Target the Anti-apoptotic Bcl-2 Family Proteins—Recent advances in cancer therapy have enabled the selective targeting of some anti-apoptotic Bcl-2 family proteins,

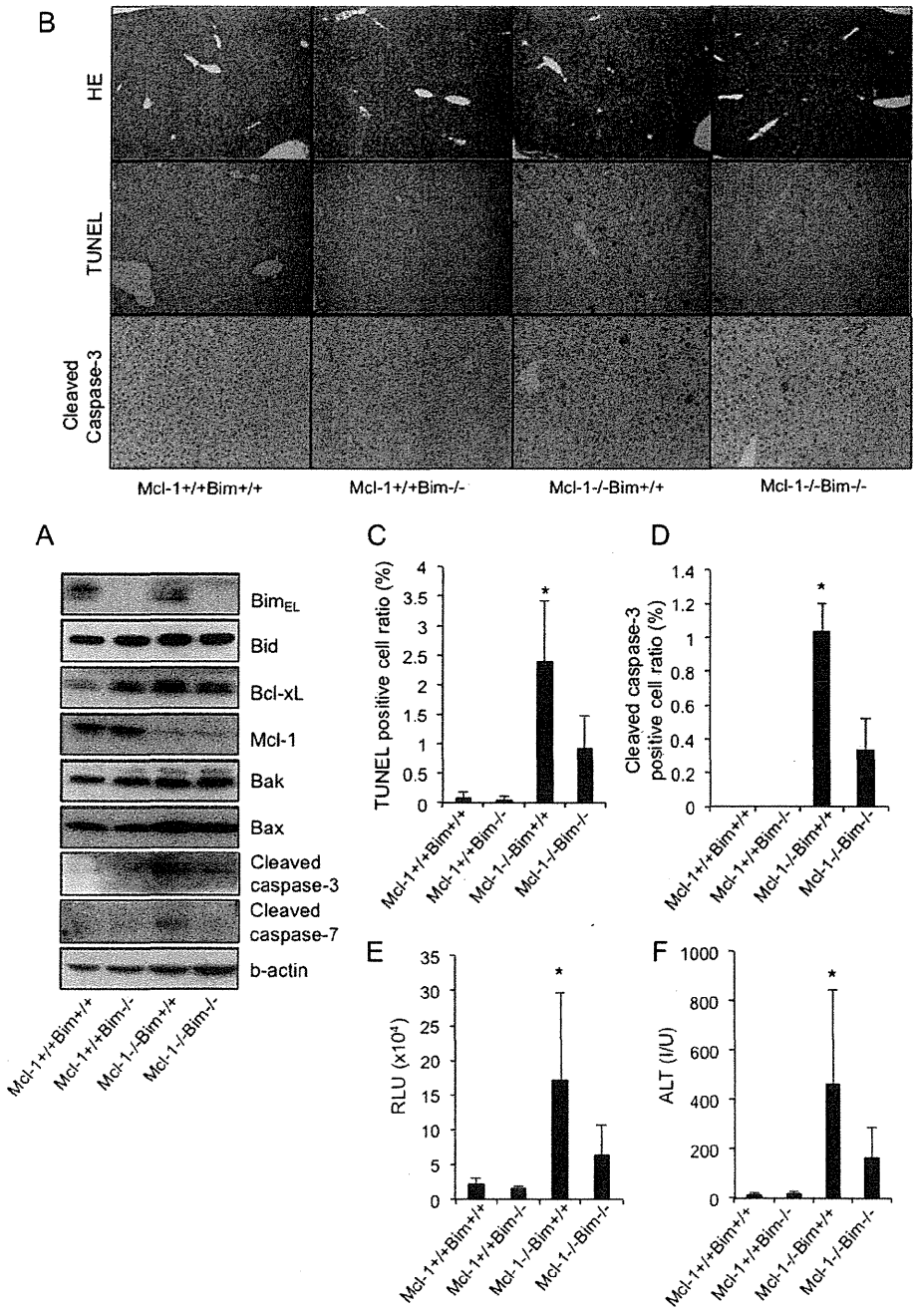

FIGURE 2. **The disruption of Bim alleviated spontaneous hepatocyte apoptosis in the absence of Mcl-1.** The offspring from the mating of *bim*$^{+-}$*mcl-1*$^{flox/flox}$*alb-cre* mice with *bim*$^{+/-}$*mcl-1*$^{flox/flox}$ mice were examined at 6 weeks of age. *Mcl-1*$^{+/+}$ and *Mcl-1*$^{-/-}$, *mcl-1*$^{flox/flox}$ and *mcl-1*$^{flox/flox}$*alb-cre*, respectively. *A*, Western blot analysis of whole liver lysates for the expression of Bim$_{EL}$, Bid, Bcl-xL, Mcl-1, Bak, Bax, cleaved caspase-3, cleaved caspse-7, and β-actin. *B*, representative images for liver histology stained with hematoxylin-eosin (*HE*), TUNEL, and cleaved caspase-3 (original magnification, ×100). *C*, TUNEL-positive cell ratio; $n = 3$–6 mice/group; *, $p < 0.05$ *versus* all. *D*, cleaved caspase-3-positive cell ratio; $n = 3$ mice/group; *, $p < 0.05$ *versus* all. *E*, serum caspase-3/7 activity; $n = 9$–15 mice/group; *, $p < 0.05$ *versus* all. *F*, serum ALT levels; $n = 9$–15 mice/group; *, $p < 0.05$ *versus* all. *Error bars*, S.D. *RLU*, relative light units; *I/U*, international units.

which are often dysregulated in malignant cells. ABT-737, which is a BH3 mimetic, could inhibit Bcl-xL, Bcl-2, and Bcl-w, and it has induced the regression of solid tumors (23). We previously reported that high dose ABT-737 administration caused hepatocyte apoptosis even in a normal liver, which was partly due to constitutive Bid-mediated BH3 stress (7). This finding led us to investigate the involvement of Bim and Bid in this ABT-737-mediated hepatotoxicity. Bim/Bid double knock-out mice (*bim*$^{-/-}$*bid*$^{-/-}$) were generated by mating Bim knock-out mice (*bim*$^{-/-}$) with Bid knock-out mice (*bid*$^{-/-}$), and the offspring were then treated with this drug. Western blot analysis confirmed the efficient deletion of Bim and Bid from the liver tissue of the double knock-out mice (Fig. 5*A*). Upon ABT-737 treatment, the Bim/Bid double knock-out mice showed complete prevention of ABT-737-induced hepatocyte apoptosis and hepatotoxicity (Fig. 5, *B*–*F*), in sharp con-

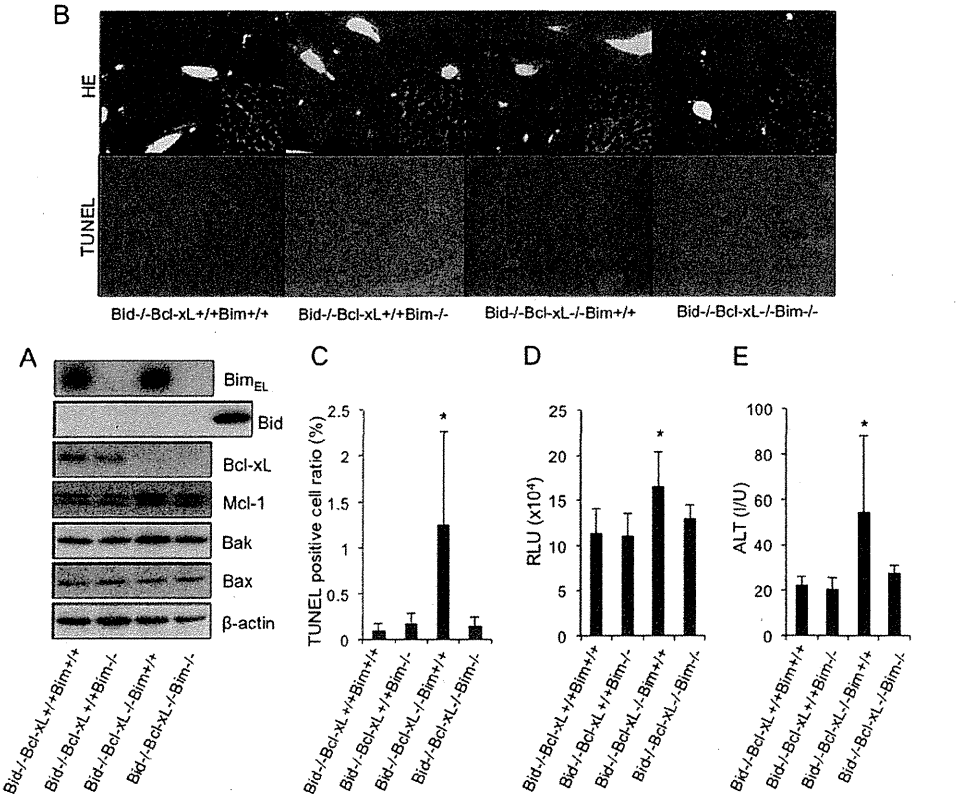

FIGURE 3. **The disruption of Bim and Bid prevented spontaneous hepatocyte apoptosis in the absence of Bcl-xL.** The offspring from the mating of *bim*$^{+/-}$*bid*$^{-/-}$*bcl-x*$^{flox/flox}$*alb-cre* mice with *bim*$^{+/-}$*bid*$^{-/-}$*bcl-x*$^{flox/flox}$ mice were examined at 6 weeks of age. *Bcl-xL*$^{+/+}$ and *Bcl-xL*$^{-/-}$, *bcl-x*$^{flox/flox}$ and *bcl-x*$^{flox/flox}$*alb-cre*, respectively. *A*, Western blot analysis of whole liver lysates for the expression of Bim$_{EL}$, Bid, Bcl-xL, Mcl-1, Bak, Bax, and β-actin. *B*, representative images of liver histology stained with hematoxylin-eosin (*HE*) and TUNEL (original magnifications, ×100 (*large panels*) and ×400 (*insets*)). *Black arrows* indicate apoptotic bodies. *C*, TUNEL-positive cell ratio; more than 5 mice/group; *, $p < 0.05$ *versus* all. *D*, serum caspase-3/7 activity; more than 6 mice/group; *, $p < 0.05$ *versus* all. *E*, serum ALT levels; more than 6 mice/group; *, $p < 0.05$ *versus* all. *Error bars*, S.D. *RLU*, relative light units; *I/U*, international units.

trast to their Bid-knock-out littermates, which still showed moderate hepatocyte apoptosis (Fig. 5, *C–E*) and increased serum ALT levels (Fig. 5*F*). These findings suggested that Bim- and Bid-mediated constant BH3 stress evoked hepatotoxicity by promoting the intrinsic pathway of apoptosis with the use of the inhibitors of the Bcl-2 family.

DISCUSSION

At least eight BH3-only proteins are known, and five have been reported to exist in hepatocytes: Bid, Bim, Noxa, Puma, and Bad (22). We also confirmed these five proteins in the liver tissue of our mice (Fig. 1*A*), and we detected at least the mRNA expression of three other genes (supplemental Fig. 1). These proteins are considered to function as pro-apoptotic sensors upon activation by a variety of apoptotic stimuli, thereby promoting an intrinsic pathway of apoptosis in a manner that is dependent on the presence of Bak and Bax. In previous studies, bile acids or death receptor stimuli activated Bid and induced liver injury, which was alleviated by Bid disruption (12, 22). Bim activation was involved in hepatocyte lipoapoptosis, which is a critical feature of non-alcoholic steatohepatitis, and in reactive oxygen species-induced hepatocyte apoptosis (10, 11, 14). Additionally, a recent *in vivo* study revealed that the activation of Bid and Bim played a central pro-apoptotic role in fatal TNF-α-induced hepatitis (24). Taken together, these findings indicated the importance of these two BH3-only proteins in the pathogenesis of various liver diseases (12, 24, 25). Conversely, the systemic knock-out of Bid or Bim in mice did not result in any liver abnormalities under normal conditions; therefore, there has not been much interest in studying their physiological involvement in the healthy liver (12, 26). However, our present study showed that spontaneous hepatocyte apoptosis in the absence of Bcl-xL was alleviated by the deletion of either Bim or Bid, and it was diminished by the deletion of both. These results indicated that these BH3-only proteins are functionally active even in the healthy liver, but they are fully restrained by the anti-apoptotic Bcl-2 family proteins in the physiological state.

What type of stimuli constitutively activate these BH3-only proteins remains unknown. The liver is a specific organ that can be continuously exposed to a variety of stimuli, such as bile acids and enteric endotoxin, as well as interactions with immune cells. These stimuli might cause constitutive BH3-only stress through the activation of death receptors, such as Fas, tumor necrosis factor (TNF), and TNF-related apoptosis-inducing ligand (TRAIL) receptors. To explore the involvement of Fas signaling in generating this BH3-only stress, we studied the effect of *fas* inhibition in the hepatocyte apoptosis induced by the genetic disruption of Bcl-xL or ABT-737 administration. siRNA-mediated *in vivo* knockdown of *fas* did not alleviate their hepatocyte apoptosis (supplemental Fig. 2, *B* and *D*), suggesting that Fas signaling may not be the origin of this BH3-only

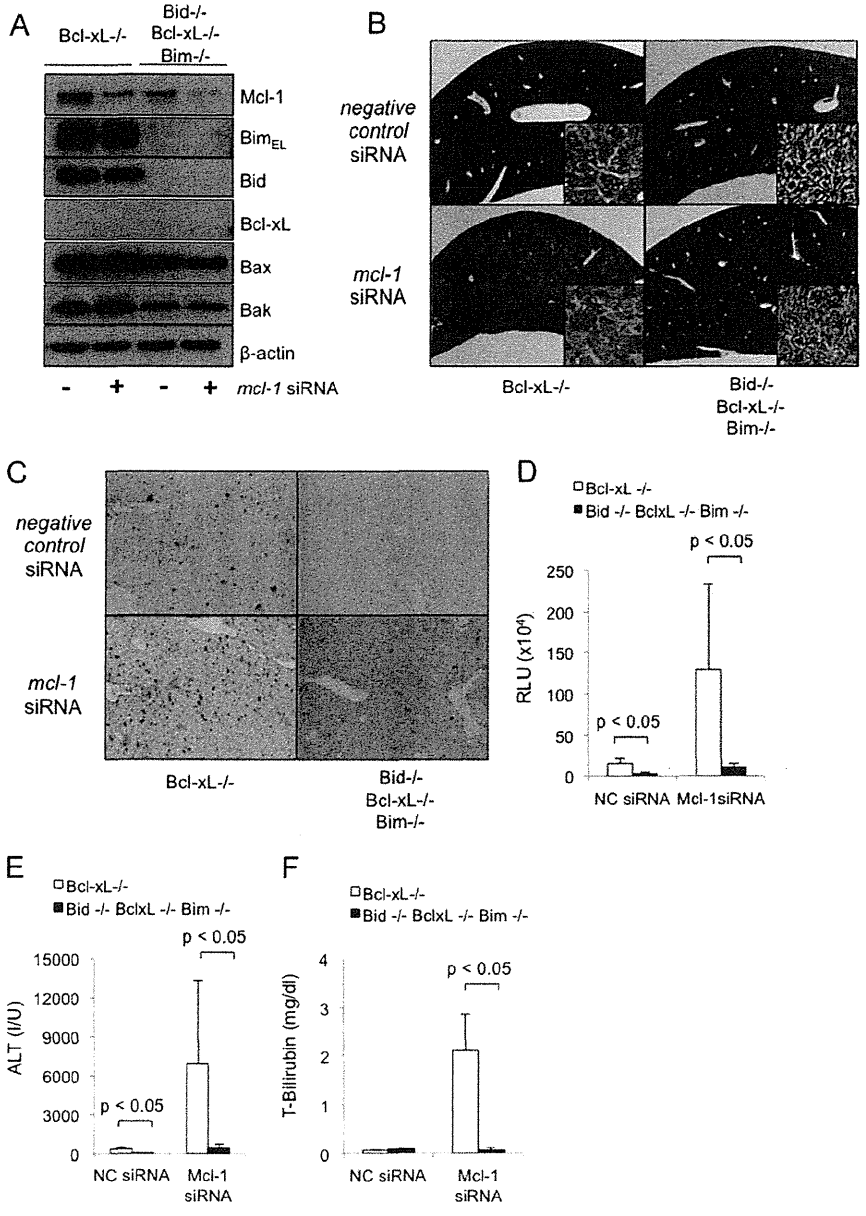

FIGURE 4. **Bim and Bid are essential regulators involved in the intrinsic pathway of apoptosis in hepatocytes in the absence of anti-apoptotic Bcl-2 family proteins.** *bcl-x$^{flox/flox}$alb-cre* mice and *bim$^{-/-}$bid$^{-/-}$bcl-x$^{flox/flox}$alb-cre* mice were injected with *mcl-1* or with negative control siRNA via the tail vein and were sacrificed 24 h (*A* and *C–F*) or 48 h (*B*) later. *Bcl-xL$^{+/+}$* and *Bcl-xL$^{-/-}$*, *bcl-x$^{flox/flox}$* and *bcl-x$^{flox/flox}$alb-cre*, respectively. *NC*, negative control. *A*, Western blot analysis of whole liver lysates for the expression of Bim$_{EL}$, Bid, Bcl-xL, Mcl-1, Bak, Bax, and β-actin. *B*, representative images of liver histology stained with hematoxylin-eosin (original magnifications, ×100 (*large panels*) and ×400 (*insets*)). *C*, representative images of liver histology stained with TUNEL (original magnification, ×100). *D*, serum caspase-3/7 activity; $n = 3–4$ mice/group. *E*, serum ALT levels; $n = 4$ mice/group; data are presented as means ± S.E. (*error bars*). *F*, serum T-bilirubin levels; $n = 4$ mice/group. *RLU*, relative light units; *I/U*, international units.

stress. However, it should be noted here that siRNA administration only decreased *fas* mRNA levels to around half (supplemental Fig. 2, *A* and *C*). Therefore, genetic study is still necessary to clarify its involvement. In order to examine the involvement of T and B cells, which comprise about 50% of intrahepatic resident immune cells (27), in producing the BH3-only stress in the healthy liver, we crossed hepatocyte-specific Mcl-1 knock-out mice with homozygous SCID mutant mice, which are characterized by an absence of functional T cells and B cells (28). The spontaneous hepatocyte apoptosis of the Mcl-1 knock-out mice was unchanged even in the homozygous SCID mutant background, monitored by serum ALT levels and serum caspase-3/7 activity (supplemental Fig. 3, *A–D*). These data indicate that these immune cells are not the major source of the BH3-only stress in the liver under physiological conditions. Therefore, further study is required to identify the main source of constitutive BH3-only stress in the healthy liver. We previously reported that Mcl-1 and Bcl-xL individually worked as apoptotic antagonists in differentiated hepatocytes (13). However, the hepatocyte-specific deletion of both led to early postnatal death due to the failure of hepatocyte development in the fetal liver (13), thus hampering the clarification of their

nized as important oncogenes (29). ABT-737, which was recently developed to inhibit the Bcl-xL, Bcl-w, and Bcl-2 proteins, displays anti-tumor activity against lymphoid malignancies and small-cell lung carcinoma (23). These drugs were considered to selectively target tumor cells because malignant cells receive many genotoxic and environmental stress-induced BH3-only signals, so these cells are thus dependent on the anti-apoptotic Bcl-2 family members for their survival. However, we previously reported that the high-dose administration of ABT-737 (100 mg/kg) elicited hepatotoxicity via Bak/Bax-dependent apoptosis in normal hepatocytes (7), suggesting that dependence on the anti-apoptotic Bcl-2 family proteins is not a specific feature of tumor cells but is the case in healthy liver cells. In the present study, we demonstrated that the disruption of Bim and Bid completely prevented hepatocyte apoptosis and hepatotoxicity induced by high dose ABT-737 (100 mg/kg), suggesting that these proteins are responsible for this hepatotoxicity. Meanwhile, although 25 mg/kg ABT-737, which is relatively close to the clinical dose, caused moderate hepatocyte apoptosis, this apoptosis was completely blocked by Bid inhibition (supplemental Fig. 4). Therefore, it is unclear whether both Bid and Bim are truly involved in hepatotoxicity when using ABT-737 at clinically relevant doses.

This study demonstrated that Bim was also involved in the hepatocyte apoptosis caused by Mcl-1 deficiency in addition to Bid, which was noted in our previous report (13). Several previous human studies have reported that Mcl-1 proteins were down-regulated in the liver tissues of non-alcoholic steatohepatitis and primary biliary cirrhosis patients (30, 31), and experimental studies have demonstrated that Mcl-1 down-regulation by saturated fatty acids caused hepatocyte lipoapoptosis, which plays an important role in the development of fatty liver disease (32, 33). Taken together with our findings, these reports suggest the possibility that Bim- and Bid-mediated constant BH3 stresses might constitute therapeutic targets of the hepatotoxicity observed in these human liver diseases.

In conclusion, we have demonstrated that the novel rheostatic balance between the pro-apoptotic BH3-only proteins Bim and Bid and the anti-apoptotic Bcl-2 family proteins Bcl-xL and Mcl-1 regulates hepatocyte life and death in the physiological state. Our present study sheds new light on the dynamic and well orchestrated Bcl-2 networks in the healthy liver.

Acknowledgments—We thank Lothar Hennighausen (National Institutes of Health) and Dr. You-Wen He (Duke University) for providing the floxed bcl-x mice and floxed mcl-1 mice, respectively. We also thank Abbott Laboratories for providing ABT-737.

REFERENCES

1. Youle, R. J., and Strasser, A. (2008) The BCL-2 protein family. Opposing activities that mediate cell death. *Nat. Rev. Mol. Cell Biol.* **9,** 47–59
2. Chipuk, J. E., and Green, D. R. (2008) How do BCL-2 proteins induce mitochondrial outer membrane permeabilization? *Trends Cell Biol.* **18,** 157–164
3. Adams, J. M., and Cory, S. (2007) Bcl-2-regulated apoptosis. Mechanism and therapeutic potential. *Curr. Opin. Immunol.* **19,** 488–496
4. Kim, H., Rafiuddin-Shah, M., Tu, H. C., Jeffers, J. R., Zambetti, G. P., Hsieh, J. J., and Cheng, E. H. (2006) Hierarchical regulation of mitochondrion-dependent apoptosis by BCL-2 subfamilies. *Nat. Cell Biol.* **8,** 1348–1358
5. Willis, S. N., Fletcher, J. I., Kaufmann, T., van Delft, M. F., Chen, L., Czabotar, P. E., Ierino, H., Lee, E. F., Fairlie, W. D., Bouillet, P., Strasser, A., Kluck, R. M., Adams, J. M., and Huang, D. C. (2007) Apoptosis initiated when BH3 ligands engage multiple Bcl-2 homologs, not Bax or Bak. *Science* **315,** 856–859
6. Korsmeyer, S. J., Shutter, J. R., Veis, D. J., Merry, D. E., and Oltvai, Z. N. (1993) Bcl-2/Bax. A rheostat that regulates an anti-oxidant pathway and cell death. *Semin. Cancer Biol.* **4,** 327–332
7. Hikita, H., Takehara, T., Kodama, T., Shimizu, S., Hosui, A., Miyagi, T., Tatsumi, T., Ishida, H., Ohkawa, K., Li, W., Kanto, T., Hiramatsu, N., Hennighausen, L., Yin, X. M., and Hayashi, N. (2009) BH3-only protein bid participates in the Bcl-2 network in healthy liver cells. *Hepatology* **50,** 1972–1980
8. Giam, M., Huang, D. C., and Bouillet, P. (2008) BH3-only proteins and their roles in programmed cell death. *Oncogene* **27,** Suppl. 1, S128–S136
9. Lomonosova, E., and Chinnadurai, G. (2008) *Oncogene* **27,** Suppl. 1, S2–S19
10. Barreyro, F. J., Kobayashi, S., Bronk, S. F., Werneburg, N. W., Malhi, H., and Gores, G. J. (2007) Transcriptional regulation of Bim by FoxO3A mediates hepatocyte lipoapoptosis. *J. Biol. Chem.* **282,** 27141–27154
11. Ishihara, Y., Takeuchi, K., Ito, F., and Shimamoto, N. (2011) Dual regulation of hepatocyte apoptosis by reactive oxygen species. Increases in transcriptional expression and decreases in proteasomal degradation of BimEL. *J. Cell Physiol.* **226,** 1007–1016
12. Yin, X. M., Wang, K., Gross, A., Zhao, Y., Zinkel, S., Klocke, B., Roth, K. A., and Korsmeyer, S. J. (1999) Bid-deficient mice are resistant to Fas-induced hepatocellular apoptosis. *Nature* **400,** 886–891
13. Hikita, H., Takehara, T., Shimizu, S., Kodama, T., Li, W., Miyagi, T., Hosui, A., Ishida, H., Ohkawa, K., Kanto, T., Hiramatsu, N., Yin, X. M., Hennighausen, L., Tatsumi, T., and Hayashi, N. (2009) Mcl-1 and Bcl-xL cooperatively maintain integrity of hepatocytes in developing and adult murine liver. *Hepatology* **50,** 1217–1226
14. Ishihara, Y., Ito, F., and Shimamoto, N. (2011) Increased expression of c-Fos by extracellular signal-regulated kinase activation under sustained oxidative stress elicits BimEL upregulation and hepatocyte apoptosis. *FEBS J.* **278,** 1873–1881
15. Malhi, H., Bronk, S. F., Werneburg, N. W., and Gores, G. J. (2006) Free fatty acids induce JNK-dependent hepatocyte lipoapoptosis. *J. Biol. Chem.* **281,** 12093–12101
16. Dzhagalov, I., St John, A., and He, Y. W. (2007) The antiapoptotic protein Mcl-1 is essential for the survival of neutrophils but not macrophages. *Blood* **109,** 1620–1626
17. Takehara, T., Tatsumi, T., Suzuki, T., Rucker, E. B., 3rd, Hennighausen, L., Jinushi, M., Miyagi, T., Kanazawa, Y., and Hayashi, N. (2004) Hepatocyte-specific disruption of Bcl-xL leads to continuous hepatocyte apoptosis and liver fibrotic responses. *Gastroenterology* **127,** 1189–1197
18. Wagner, K. U., Claudio, E., Rucker, E. B., 3rd, Riedlinger, G., Broussard, C., Schwartzberg, P. L., Siebenlist, U., and Hennighausen, L. (2000) Conditional deletion of the Bcl-x gene from erythroid cells results in hemolytic anemia and profound splenomegaly. *Development* **127,** 4949–4958
19. Maruyama, C., Suemizu, H., Tamamushi, S., Kimoto, S., Tamaoki, N., and Ohnishi, Y. (2002) Genotyping the mouse severe combined immunodeficiency mutation using the polymerase chain reaction with confronting two-pair primers (PCR-CTPP). *Exp. Anim.* **51,** 391–393
20. Kodama, T., Takehara, T., Hikita, H., Shimizu, S., Shigekawa, M., Tsunematsu, H., Li, W., Miyagi, T., Hosui, A., Tatsumi, T., Ishida, H., Kanto, T., Hiramatsu, N., Kubota, S., Takigawa, M., Tomimaru, Y., Tomokuni, A., Nagano, H., Doki, Y., Mori, M., and Hayashi, N. (2011) Increases in p53 expression induce CTGF synthesis by mouse and human hepatocytes and result in liver fibrosis in mice. *J. Clin. Invest.* **121,** 3343–3356
21. Kodama, T., Takehara, T., Hikita, H., Shimizu, S., Li, W., Miyagi, T., Hosui, A., Tatsumi, T., Ishida, H., Tadokoro, S., Ido, A., Tsubouchi, H., and Hayashi, N. (2010) Thrombocytopenia exacerbates cholestasis-induced liver fibrosis in mice. *Gastroenterology* **138,** 2487–2498, 2498.e2481–2487
22. Baskin-Bey, E. S., and Gores, G. J. (2005) Death by association. BH3 domain-only proteins and liver injury. *Am. J. Physiol. Gastrointest. Liver Physiol.* **289,** G987–G990
23. Oltersdorf, T., Elmore, S. W., Shoemaker, A. R., Armstrong, R. C., Augeri,

D. J., Belli, B. A., Bruncko, M., Deckwerth, T. L., Dinges, J., Hajduk, P. J., Joseph, M. K., Kitada, S., Korsmeyer, S. J., Kunzer, A. R., Letai, A., Li, C., Mitten, M. J., Nettesheim, D. G., Ng, S., Nimmer, P. M., O'Connor, J. M., Oleksijew, A., Petros, A. M., Reed, J. C., Shen, W., Tahir, S. K., Thompson, C. B., Tomaselli, K. J., Wang, B., Wendt, M. D., Zhang, H., Fesik, S. W., and Rosenberg, S. H. (2005) An inhibitor of Bcl-2 family proteins induces regression of solid tumours. *Nature* **435,** 677–681

24. Kaufmann, T., Jost, P. J., Pellegrini, M., Puthalakath, H., Gugasyan, R., Gerondakis, S., Cretney, E., Smyth, M. J., Silke, J., Hakem, R., Bouillet, P., Mak, T. W., Dixit, V. M., and Strasser, A. (2009) Fatal hepatitis mediated by tumor necrosis factor TNFα requires caspase-8 and involves the BH3-only proteins Bid and Bim. *Immunity* **30,** 56–66
25. Higuchi, H., Miyoshi, H., Bronk, S. F., Zhang, H., Dean, N., and Gores, G. J. (2001) Bid antisense attenuates bile acid-induced apoptosis and cholestatic liver injury. *J. Pharmacol. Exp. Ther.* **299,** 866–873
26. Bouillet, P., Metcalf, D., Huang, D. C., Tarlinton, D. M., Kay, T. W., Köntgen, F., Adams, J. M., and Strasser, A. (1999) Proapoptotic Bcl-2 relative Bim required for certain apoptotic responses, leukocyte homeostasis, and to preclude autoimmunity. *Science* **286,** 1735–1738
27. Blom, K. G., Qazi, M. R., Matos, J. B., Nelson, B. D., DePierre, J. W., and Abedi-Valugerdi, M. (2009) Isolation of murine intrahepatic immune cells employing a modified procedure for mechanical disruption and functional characterization of the B, T, and natural killer T cells obtained. *Clin. Exp. Immunol.* **155,** 320–329
28. Shultz, L. D., Schweitzer, P. A., Christianson, S. W., Gott, B., Schweitzer, I. B., Tennent, B., McKenna, S., Mobraaten, L., Rajan, T. V., and Greiner, D. L. (1995) Multiple defects in innate and adaptive immunologic function in NOD/LtSz-scid mice. *J. Immunol.* **154,** 180–191
29. Kirkin, V., Joos, S., and Zörnig, M. (2004) The role of Bcl-2 family members in tumorigenesis. *Biochim. Biophys. Acta* **1644,** 229–249
30. García-Monzon, C., Lo Iacono, O., Mayoral, R., González-Rodriguez, A., Miquilena-Colina, M. E., Lozano-Rodríguez, T., García-Pozo, L., Vargas-Castrillón, J., Casado, M., Boscá, L., Valverde, A. M., and Martín-Sanz, P. (2011) Hepatic insulin resistance is associated with increased apoptosis and fibrogenesis in nonalcoholic steatohepatitis and chronic hepatitis C. *J. Hepatol.* **54,** 142–152
31. Iwata, M., Harada, K., Kono, N., Kaneko, S., Kobayashi, K., and Nakanuma, Y. (2000) Expression of Bcl-2 familial proteins is reduced in small bile duct lesions of primary biliary cirrhosis. *Hum. Pathol.* **31,** 179–184
32. Ibrahim, S. H., Kohli, R., and Gores, G. J. (2011) Mechanisms of lipotoxicity in NAFLD and clinical implications. *J. Pediatr. Gastroenterol. Nutr.* **53,** 131–140
33. Masuoka, H. C., Mott, J., Bronk, S. F., Werneburg, N. W., Akazawa, Y., Kaufmann, S. H., and Gores, G. J. (2009) Mcl-1 degradation during hepatocyte lipoapoptosis. *J. Biol. Chem.* **284,** 30039–30048

Research Article

EASL EUROPEAN ASSOCIATION FOR THE STUDY OF THE LIVER | JOURNAL OF HEPATOLOGY

Carbamazepine promotes liver regeneration and survival in mice

Tsukasa Kawaguchi†, Takahiro Kodama†, Hayato Hikita, Satoshi Tanaka, Minoru Shigekawa, Takatoshi Nawa, Satoshi Shimizu, Wei Li, Takuya Miyagi, Naoki Hiramatsu, Tomohide Tatsumi Tetsuo Takehara*

Department of Gastroenterology and Hepatology, Osaka University Graduate School of Medicine, Suita, Osaka 565-0871, Japan

Background & Aims: Carbamazepine (CBZ), a widely used anticonvulsant and mood stabilizer, activates multiple proliferative and pro-survival pathways. Here, we hypothesize that CBZ may promote hepatocellular proliferation and ameliorate liver regeneration.

Methods: C57BL6/J mice were orally administered CBZ or vehicle and underwent a 70% partial hepatectomy (PHx), 85% PHx or treatment with carbon tetrachloride (CCl_4). Liver regeneration was determined by liver to body weight ratio, hepatocyte proliferation markers, and activation of intracellular signalling pathways.

Results: Two to 5 days after the 70% PHx, the liver to body weight ratio was significantly higher in the CBZ-treated mice than in the vehicle-treated mice. CBZ treatment upregulated the number of proliferative hepatocytes following PHx or CCl_4 treatment, as assessed by intrahepatic Ki-67 staining, BrdU uptake, and PCNA protein expression. PHx surgery induced the expression of several cyclins and activated Akt/mTOR signalling pathways, all of which were enhanced by CBZ treatment. The administration of the mTOR inhibitor temsirolimus abrogated the hepato-proliferative effect of CBZ. CBZ treatment significantly improved the survival rate of the mice that underwent lethal 85% massive hepatectomy.

Conclusions: CBZ demonstrated a novel hepato-proliferative effect through the activation of the mTOR signalling pathway in hepatectomised mice. CBZ has the potential to be a therapeutic option for facilitating efficient liver regeneration in patients subjected to liver surgery.

Keywords: Carbamazepine; Liver regeneration; Hepatocyte proliferation; Akt; mTOR.

Received 25 December 2012; received in revised form 3 July 2013; accepted 5 July 2013; available online 18 July 2013

* Corresponding author. Address: Department of Gastroenterology and Hepatology, Osaka University Graduate School of Medicine, 2-2 Yamada-oka, Suita, Osaka 565-0871, Japan. Tel.: +81 6 6879 3621; fax: +81 6 6879 3629.

E-mail address: takehara@gh.med.osaka-u.ac.jp (T. Takehara).

† These authors contributed equally to this work and share first authorship.

Abbreviations: CBZ, carbamazepine; PHx, partial hepatectomy; PI-3K, phosphotidylinositol-3 kinase; MAPK, ras-mitogen-activated protein kinase; ERK, extracellular signal regulated kinase; DMSO, dimethyl sulfoxide; H&E, haematoxylin and eosin; IHC, immunohistochemistry; RT-PCR, reverse transcription PCR; JNK, c-jun N-terminal kinase; CCl_4, carbon tetrachloride; NPC, non-parenchymal cells; HGF, hepatocyte growth factor.

Introduction

Hepatocyte proliferation is critically important in liver regeneration after surgical resection or living donor transplantation. It involves the recovery from loss of volume and impaired liver function [1–3]. If this fundamental proliferative ability is not sufficient to compensate for the resected liver, postoperative liver failure will occur, which is a serious complication and remains an important clinical problem [4,5]. To overcome this issue, therapeutic methods that support liver regeneration must be explored. However, few treatment options are capable of enhancing liver regeneration in a clinical setting, despite widespread interest and numerous trials [6,7]. Carbamazepine (CBZ) is FDA-approved and widely used as an anticonvulsant or a mood stabiliser in clinical settings [8,9]. Mood stabilisers have been shown to exert prosurvival and cytoprotective effects on neuronal cells through the activation of intracellular signalling pathways that involve the phosphotidylinositol-3 kinase (PI-3K)-Akt pathway and the Ras-mitogen-activated protein kinase (MAPK) cascade [10–12]. In fact, CBZ induces a rapid and prolonged phosphorylation of extracellular signal regulated kinase (ERK) in human neuroblastoma cells [13]. In addition to the close relationship of CBZ to prosurvival signalling, a recent report revealed the therapeutic potential of CBZ in treating liver fibrosis caused by α1-antitrypsin deficiency, one of the chronic liver diseases leading to cirrhosis and liver failure [14]. These findings fascinated us enough to encourage the evaluation of the favourable effect of CBZ on liver regeneration after surgical resection. In the present study, we identified a novel hepato-proliferative effect of CBZ on hepatectomised mice that is mediated through the activation of the mTOR pathway. This effect could partially protect the mice against the high lethality associated with massive liver resection. These results imply the therapeutic potential of CBZ to support liver regeneration in patients who are subjected to liver resection or living donor transplantation.

Materials and methods

Mice

Six- to eight-week-old male C57BL/6J mice were purchased from Charles River Laboratories Japan (Tokyo). The mice were maintained in a specific pathogen-free facility with a 12-hour-dark/12-hour-light cycle and received humane treatment. All animal-related procedures were approved by the Animal Care and Use committee of Osaka University Medical School.

Surgery and materials

The mice were anesthetised with inhaled isoflurane and subjected to sham operation or 70% partial hepatectomy (PHx) as previously described (n >3 for each group and time point) [15]. Then, the mice were euthanized at indicated time points after surgery. The 85% PHx surgical procedure was identical to 70% PHx but with the additional resection of the right lower and caudate lobes [16]. Carbamazepine (CBZ) was purchased from Sigma-Aldrich (St. Louis, MO) and dissolved in a stock solution of 50 mg/ml dimethyl sulfoxide (DMSO). The mice were orally administered 250 mg/kg of CBZ or an equivalent volume of DMSO 2 h before surgery. The CBZ dosage was determined based on a previous *in vivo* study [14]. Temsirolimus was purchased from Sigma-Aldrich and dissolved in a stock solution of 20 mg/ml DMSO. The mice were injected intraperitoneally with 5 mg/kg of temsirolimus or an equivalent volume of DMSO 4 h before surgery. The temsirolimus dosage was determined based on a previous *in vivo* study reporting its inhibitory effects on mTOR [17].

Blood tests

To measure serum AST and ALT levels, blood was collected from the inferior vena cava of mice and centrifuged at 10,000g at room temperature for 15 min. Serum AST and ALT levels were measured by a standard method at the Oriental Kobo Life Science Laboratory (Nagahama, Japan).

Histological analyses

The dissected livers were fixed in formalin and embedded in paraffin. The sections were stained with haematoxylin and eosin (H&E). To assess hepatocyte proliferation, the sections were further processed for immunohistochemistry (IHC) with anti-Ki-67 antibody (Sigma-Aldrich) and anti-PCNA antibody (Cell Signaling Technology, Beverly MA). For IHC, antigen retrieval was performed by steaming for 20 min in 1× Target Retrieval Solution (pH 6.0) (DAKO, Glostrup, Denmark). The quenching of the endogenous peroxidase was accomplished with a 10-min incubation in 3% hydrogen peroxide in methanol. Sections were stained using the immunoperoxidase technique and counterstained with haematoxylin. We also stained liver sections for nuclear BrdU incorporation as previously described [18].

Western blot analysis

A piece of frozen liver tissue was lysed in lysis buffer (1% NP-40, 0.5% sodium deoxycholate, 0.1% sodium dodecyl sulphate, 1× protease inhibitor cocktail [Nacalai Tesque, Kyoto Japan], 1× phosphatase inhibitor cocktail [Nacalai Tesque], phosphate-buffered saline, pH7.4). The homogenates were purified by centrifugation at 10,000*g* at 4 °C for 15 min. The protein concentrations were determined using a bicinchoninic acid protein assay (Thermo Scientific, Rockford, IL). Equal amounts of protein extract were electrophoretically separated by SDS polyacrylamide gels and transferred onto a polyvinylidene fluoride membrane. For immunodetection, the following antibodies were used: anti-cyclinE1, anti-Akt, anti-phospho Akt (Thr 308), anti-phospho Akt (Ser 473), anti-mTOR, anti-phospho mTOR (Ser 2448), anti-S6K, anti-phospho S6K (Thr 389), anti-4EBP1, anti-phospho-4EBP1 (Thr 37/46), anti-ERK, and anti-phospho ERK (Thr 202/Tyr 204), anti-JNK, anti-phospho JNK (Thr 183/Tyr 185) (Cell Signaling Technology), anti-cyclinA (Santa Cruz Biotechnology Inc., Santa Cruz, CA), PCNA and β-actin (Sigma-Aldrich).

Real-time quantitative PCR

Total RNA isolated from liver tissues using an RNeasy Mini Kit (QIAGEN) was reverse transcribed and subjected to real-time reverse transcription PCR (RT-PCR) as previously described [18]. The mRNA expression levels of the specific genes were quantified using TaqMan Gene Expression Assays (Applied Biosystems) as follows: murine *ccna2* (assay ID:Mm00438063_m1), murine *ccne2* (assay ID: Mm00438077_m1), murine *hgf* (assay ID:Mm01135193_m1), murine *il6* (assay ID:Mm00446190_m1) and murine *actb* (assay ID:Mm00607939_s1). The transcript levels are presented as fold change relative to the controls.

Statistics

Data are expressed as mean ± SD. Statistical analyses between two groups were performed by an unpaired Student's *t* test unless otherwise indicated. Multiple comparisons were performed by a one-way ANOVA, and differences in the mean values among groups were examined by a Fischer *post hoc* correction. *p* values less than 0.05 were considered to be statistically significant.

Results

CBZ promotes liver regeneration after PHx

To test whether CBZ has any effect on liver regeneration, male C57BL6/J mice were orally administered CBZ or vehicle and underwent 70% PHx. The PHx procedure allows for a well-established liver regeneration model in which the liver recovers full volume after surgery. In the sham-operated mice, no difference was found in liver to body weight ratio at 48 h after drug administration between the CBZ-treated and vehicle-treated groups (Supplementary Fig. 1). In the hepatectomised mice, the ratio was significantly higher in the CBZ-treated group than in the vehicle-treated group (Supplementary Fig. 1). We then examined the liver to body weight ratio at several time points after surgery with or without one-time oral CBZ administration. After PHx, the liver to body weight ratio was rapidly recovered in the CBZ-treated mice and was significantly higher than in the vehicle-treated mice at 2, 3 and 5 days after PHx (Fig. 1A). The liver to body weight ratio reached similar levels by 14 days after surgery in both groups (Fig. 1A). These findings demonstrate that CBZ promoted liver regeneration after PHx in mice.

CBZ enhances hepatocyte proliferation after PHx

During liver regeneration, hepatocyte proliferation is critically important in compensating for the lost liver mass and liver function recovery. To determine whether CBZ affects hepatocyte proliferation in the hepatectomised mice, hepatocyte DNA synthesis was assessed by immunohistochemical staining of liver sections with Ki-67 and BrdU—two principal markers of DNA replication. We first confirmed that there was no difference in liver injury after PHx in the CBZ- or vehicle-treated mice, by evaluation of serum AST and ALT levels (Fig. 1B and C). H&E staining also revealed that there was no inflammatory cell infiltration or necrosis in the livers of either group (Fig. 1D). The number of Ki-67 positive cells increased to a peak at 48 h after PHx in both groups (Fig. 1E and F), but the peak value was significantly higher in the CBZ-treated livers (Fig. 1E and F). Similarly, the number of BrdU-positive nuclei was also significantly higher in CBZ-treated mice than in vehicle-treated mice at 36 h after PHx (Fig. 1G and H). Western blotting indicated higher protein expression levels for proliferating nuclear antigen (PCNA), another well-known marker of DNA replication, in CBZ-treated livers at 48 h after PHx (Fig. 1I). These findings indicate that CBZ increased the number of proliferative hepatocytes after PHx in mice. We also observed the similar hepato-proliferative effect and amelioration of liver regeneration in hepatectomized mice even after repeated CBZ administration for 3 consecutive days (Supplementary Fig. 2A and B), which is a more clinically relevant regimen since CBZ requires multiple administrations to reach steady state levels [19]. To determine whether this favourable effect of CBZ is only observed in a resected liver, CBZ-treated mice were administered a single injection of carbon tetrachloride (CCl_4), which causes acute liver injury, and followed compensative liver regeneration [20]. CBZ treatment did not affect the liver damage but enhanced hepatocyte proliferation (Supplementary Fig. 3A–C) suggesting that the hepato-proliferative effect of CBZ may not be limited to the hepatectomised liver.

We then examined the gene expression of several cyclins, accelerators of cell cycle progression, which are important for hepatocyte proliferation in regenerating livers [21]. A real-time RT-PCR analysis revealed that the mRNA levels of *ccne2* and *ccna2* were significantly higher in CBZ-treated mice than in

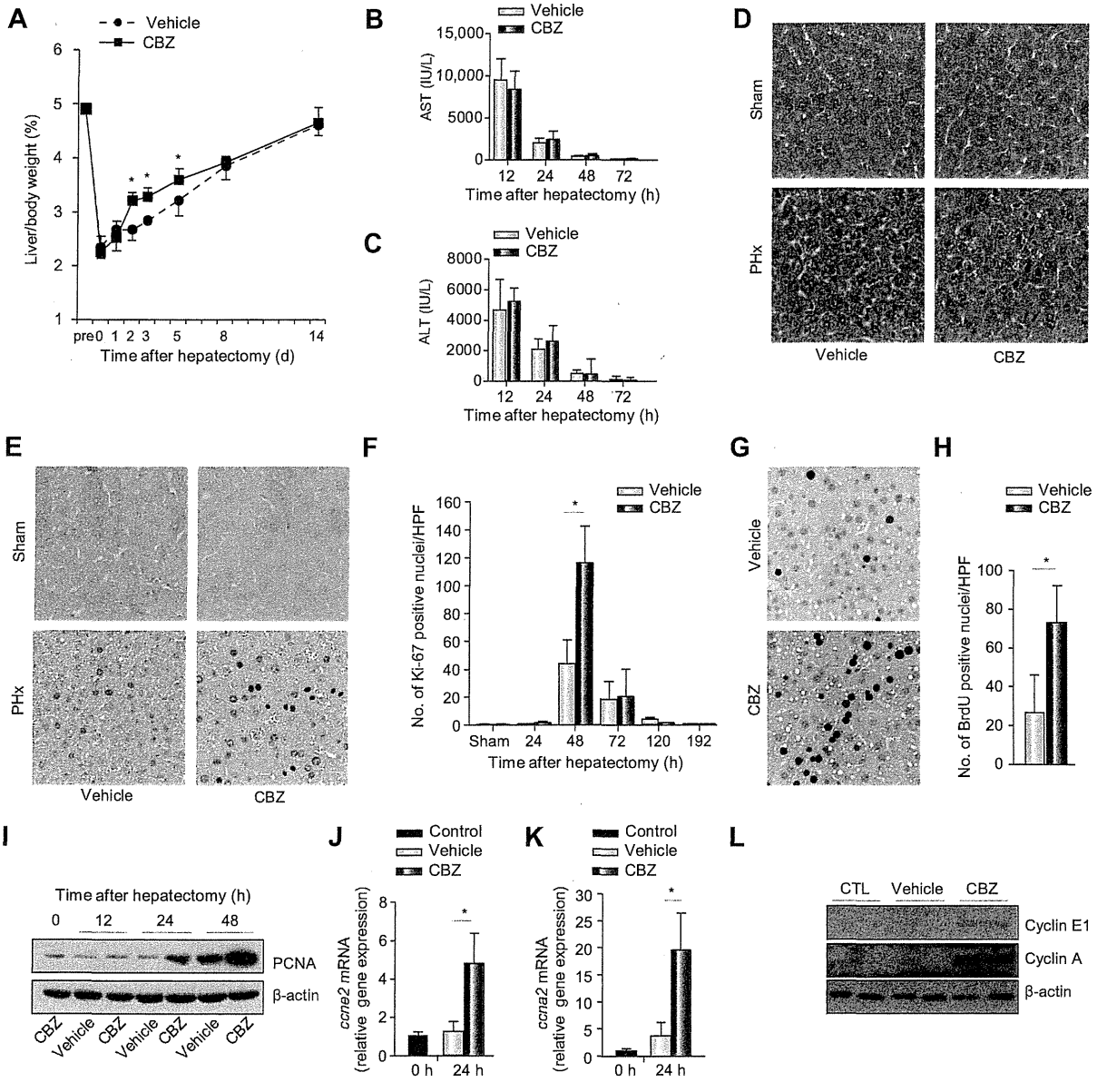

Fig. 1. CBZ promotes liver/body weight ratio recovery and enhances hepatocyte proliferation after 70% partial hepatectomy. Mice were administered 250 mg/kg of CBZ or DMSO orally and subjected to 70% partial hepatectomy 2 h later (3 mice per group). CBZ, PHx, and CTL stand for carbamazepine, 70% partial hepatectomy and control, respectively. (A) Changes in liver/body weight ratio over time in mice receiving PHx with vehicle or CBZ, *p <0.05 *vs.* vehicle. (B and C) Serum AST (B) and ALT (C) levels in vehicle- or CBZ-treated mice. (D) Liver sections at 48 h after PHx or sham operation were stained with H&E; original magnification, 400×. (E) Liver sections after surgery were evaluated for hepatocyte proliferation with anti-Ki-67 staining; original magnification, 400×. (F) The number of Ki-67 positive nuclei/high-power field (HPF) at 48 h after surgery in sham-operated mice and at indicated time in hepatectomised mice with vehicle or CBZ treatment. Six fields of view (FOVs) were counted in liver sections of individual mice, *p <0.05. (G) Liver sections at 36 h after PHx were stained with BrdU; original magnification, 400×. (H) The number of BrdU positive nuclei/HPF at 36 h after PHx in vehicle-treated and CBZ-treated mice. Six FOVs were counted in liver sections of individual mice, *p <0.05. (I) Expression of PCNA protein in liver tissue from vehicle- or CBZ-treated mice after PHx was assessed by Western blot analysis. (J and K) *ccne2* (J) and *ccna2* (K) mRNA levels in the liver were determined by real time RT-PCR at 24 h after PHx, *p <0.05. (L) Protein expression of cyclin E1 and cyclin A in liver tissue was assessed by Western blot analysis at 24 h after PHx.

vehicle-treated mice at 24 h after PHx (Fig. 1J and K). Evaluation by Western blot also demonstrated that protein levels of cyclin E1 and cyclin A were increased in CBZ-treated mice (Fig. 1L). Collectively, these results suggest that CBZ upregulated the cyclin levels in remnant hepatocytes, leading to an increase in the number of hepatocytes entering the cell cycle after PHx.

CBZ strongly activates the Akt-mTOR pathway after PHx

Mood stabilisers, including CBZ, have been reported to modulate the Akt and MAPK pathways [10–13], both of which are also involved in initiating the cell cycle progression of remaining liver cells upon liver resection [22–25]. Thus, we examined the effect

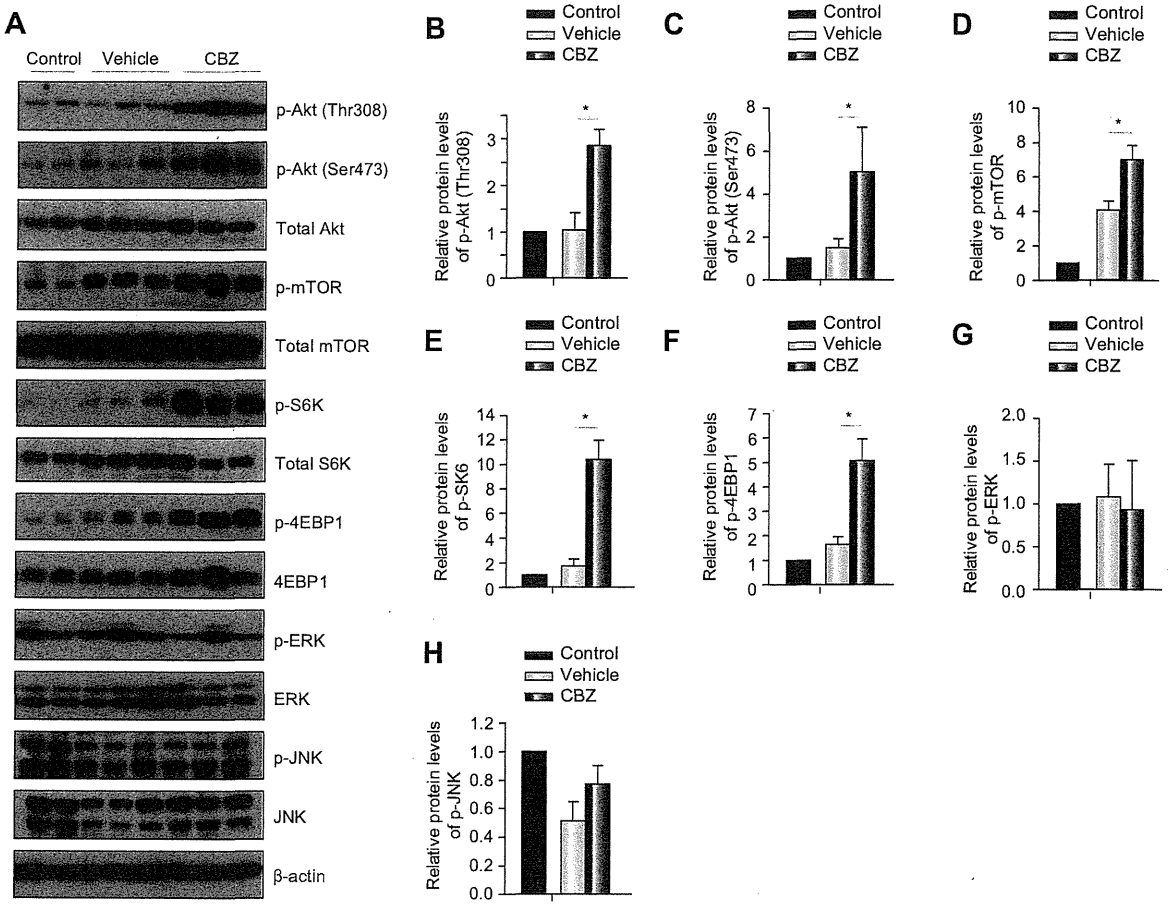

Fig. 2. CBZ strongly activates Akt-mTOR signalling. Mice were administered 250 mg/kg of CBZ or DMSO orally and subjected to 70% partial hepatectomy 2 h later (4 mice per group). (A) The phosphorylation status of Akt, mTOR, S6K, 4EBP1, ERK and JNK was assessed by Western blot analysis at 12 h after PHx. (B–H) Relative expression levels of phosphorylated proteins were calculated as the optical densities of their blots normalized to the β-actin blots; p-Akt (Thr308) (B), p-Akt (Ser473) (C), p-mTOR (D), p-S6 K (E), p-4EBP1 (F), p-ERK (G) and p-JNK (H). CBZ, carbamazepine; *p <0.05.

of CBZ on the activation of these two pathways in the livers of hepatectomised mice. PHx induced phosphorylation of Akt (Thr308, Ser473) and activated its downstream effectors, mTOR, S6K, and 4EBP1, at 12 h after surgery. All of these signalling molecules were enhanced by CBZ treatment (Fig. 2A–F). By contrast, the phosphorylation of ERK was not different between the CBZ-treated and vehicle-treated mice (Fig. 2A and G). We also evaluated the activation of the c-jun N-terminal kinase (JNK) pathway, which is closely related to liver regeneration [26], and found no difference between the two groups (Fig. 2A and H).

Activation of the mTOR pathway is responsible for enhanced hepatocyte proliferation in hepatectomised mice following CBZ treatment

To investigate whether the strong activation of Akt-mTOR pathway was ascribable to the hepato-proliferative effect of CBZ after PHx, we blocked mTOR signalling by the use of the mTOR inhibitor temsirolimus. Temsirolimus administration blocked the enhancement of mTOR pathway activation in the CBZ-treated hepatectomised livers to a level similar to the vehicle-treated hepatectomised liver (Fig. 3A), while phosphorylation of Akt, an upstream signalling molecule of mTOR, was upregulated in both mice likely due to a compensative response (Fig. 3A). Under these conditions, temsirolimus abrogated the upregulation of *ccne2* and *ccna2* mRNA expression and PCNA protein expression in the CBZ-treated hepatectomised mice (Fig. 3B–E), suggesting that the hepato-proliferative effect of CBZ is attributable to the enhanced activation of the mTOR pathway. In addition, mTOR inhibition also prevented CBZ-induced acceleration of liver mass recovery 48 h after PHx (Fig. 3F). Altogether, these findings indicate that, following PHx surgery, CBZ treatment potentiated the activation of the mTOR pathway, which enhanced hepatocyte proliferation and promoted liver regeneration.

CBZ improves the survival rate of mice that undergo 85% massive hepatectomy

Finally, we evaluated the therapeutic significance of CBZ in regeneration of the resected liver using a severe 85% massive hepatectomy model. This PHx model typically presents extremely high mortality (82%) within 2 days after surgery [27]. Consistent

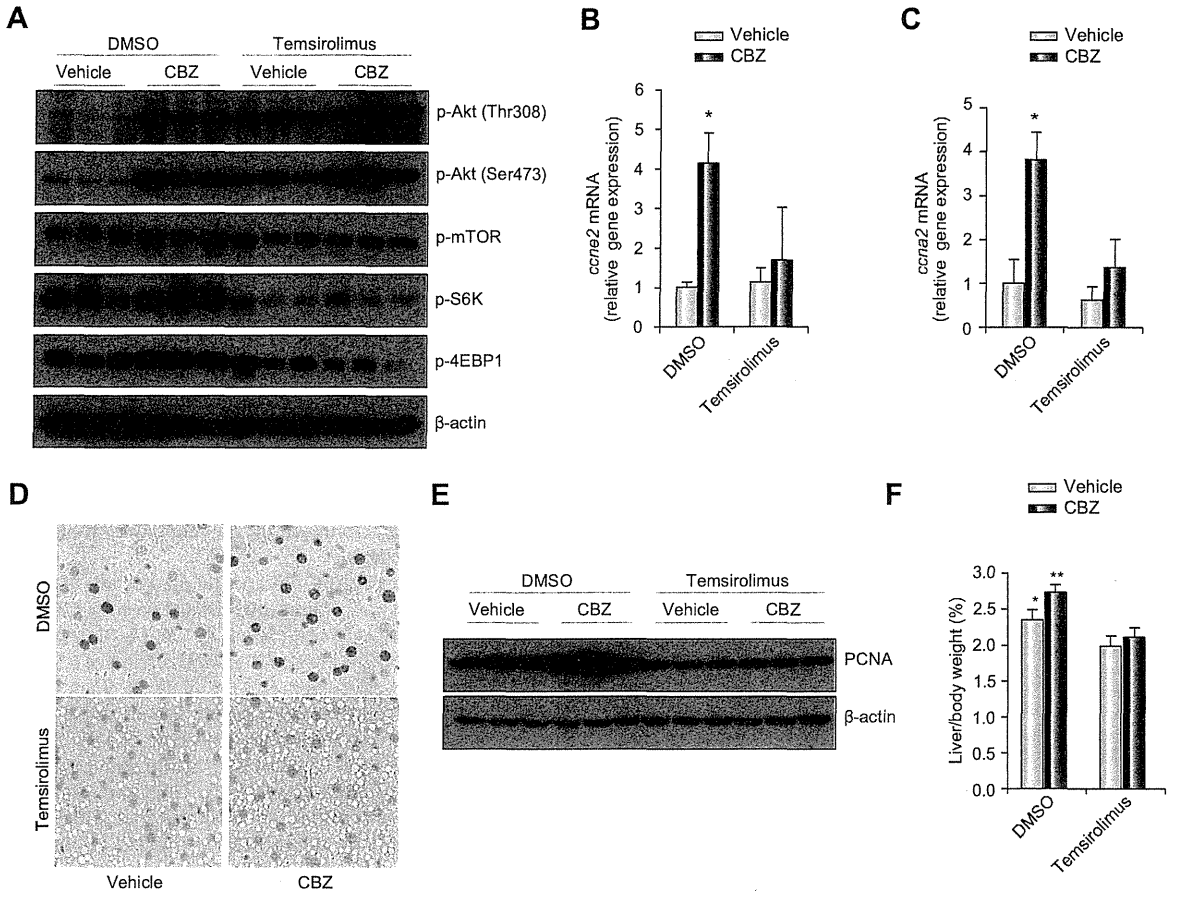

Fig. 3. mTOR inhibitor abrogates the hepato-proliferative effect of CBZ in hepatectomised mice. Mice were injected with temsirolimus or DMSO 4 h before PHx and orally administered 250 mg/kg of CBZ or DMSO 2 h before PHx. Then, mice were subjected to 70% partial hepatectomy and euthanized at indicated time points. (A) The phosphorylation status of Akt, mTOR, S6K, and 4EBP1 at 12 h after PHx was assessed by Western blot analysis. (B and C) Real-time RT-PCR analysis of *ccne2* (B) and *ccna2* (C) mRNA expression at 24 h after PHx, $^{*}p < 0.05$ *vs.* all. (D and E) The expression of PCNA proteins at 48 h after PHx was assessed by (D) immunohistochemistry and (E) Western blot analysis. (F) Liver/body weight ratio at 48 h after PHx in indicated groups. CBZ, carbamazepine; 3 mice per group. Statistical analyses were performed by one-way ANOVA. $^{*}p < 0.05$ *vs.* temsirolimus-vehicle group; $^{**}p < 0.05$ *vs.* all.

with the effect of CBZ observed in the 70% PHx model, CBZ did not affect liver injury but enhanced hepatocyte proliferation in the liver after the 85% PHx (Fig. 4A and B). Consequently, while only 4 of the 25 vehicle-treated mice survived for 7 days after 85% PHx, 11 of 25 CBZ-treated mice were alive at 7 days. The CBZ-treated mice survival rate was significantly higher than that of vehicle-treated mice (44% *vs.* 16%, $p < 0.05$) (Fig. 4C).

Discussion

Liver regeneration after surgical resection or injury is a complex phenomenon primarily dependent on hepatocyte proliferation. In the present study, we identified a new aspect of CBZ, increasing hepatocyte proliferation after partial resection of the liver in mice. We also clarified the involvement of the mTOR signalling pathway in this hepato-proliferative effect. mTOR and its downstream effectors S6K and 4EBP1, all of which were intensively upregulated by CBZ treatment, have been shown to stimulate cell cycle progression via modulation of the expression of several cyclins, such as cyclin E and cyclin A [28]. In fact, in our hepatectomised mice, CBZ enhanced upregulation of their mRNA levels, which were dependent on mTOR activation. These findings suggest that mTOR activation may produce a profound effect on cell cycle progression via upregulating cyclin expression in CBZ-treated remnant livers. In this study, we also found that CBZ enhanced Akt phosphorylation following PHx, which might be an event that is upstream of mTOR activation. As mood stabilising drugs have been described to trigger activation of PI-3K and subsequent phosphorylation of Akt in neuronal cells by generating lipid second messengers (i.e., PI-3,4,5-P3 or PI-3,4-P2) [10,13], such a mechanism might be relevant to CBZ-mediated Akt activation in resected livers. Further studies are necessary to elucidate the exact mechanism by which CBZ activates the mTOR signalling pathway.

Given that CBZ has complicated pharmacokinetic properties, a variety of mechanisms other than those involving the mTOR pathway could be related to the enhanced liver regeneration in

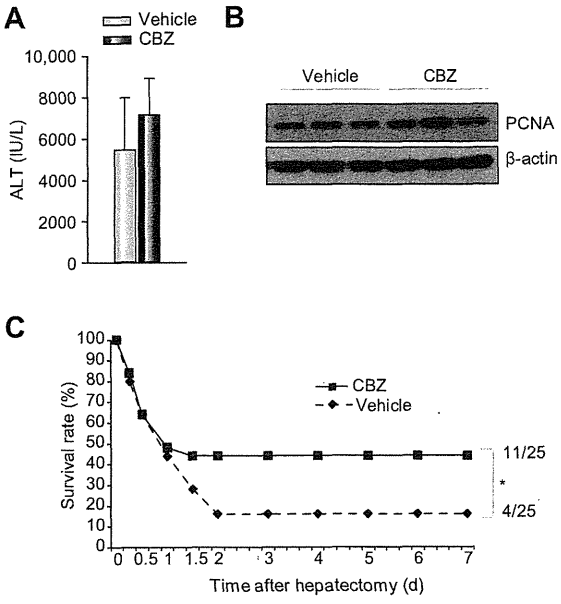

Fig. 4. CBZ improves survival of mice that undergo 85% massive hepatectomy. Mice were orally administered 250 mg/kg of CBZ or DMSO and subjected to 85% partial hepatectomy 2 h later. (A and B) Mice were euthanized 24 h after PHx (4 mice per group). (A) Serum ALT levels. (B) Expression of PCNA protein in liver tissue from vehicle- or CBZ-treated mice was assessed by Western blot analysis. (C) The survival rate was assessed at 7 days after surgery (25 mice per group). Statistical analysis was performed using Chi-square test. CBZ, carbamazepine; *p <0.05.

CBZ-treated mice. To further investigate underlying mechanisms, we performed microarray analysis of the mouse liver tissues collected after CBZ administration. Pathway analysis of microarray data revealed activation of PXR/RXR and FXR/RXR pathways (data not shown), both of which have been reported to be involved in liver regeneration [29–31]. These pathways might be also involved in the hepato-proliferative effect of CBZ.

Following PHx, both hepatocytes and non-parenchymal cells (NPCs) are activated and integrate multiple signals originating from immune, hormonal, and metabolic networks to induce hepatocyte proliferation [24]. In particular, after PHx, hepatic stellate cells and Kupffer cells produce hepatocyte growth factor (HGF) and IL-6, respectively, both of which contribute to liver regeneration partially through modulating the intrahepatic signalling pathways focused on in this study [3,32]. Therefore, we investigated the involvement of NPCs in the CBZ-induced hepato-proliferative effect in hepatectomised mice. Neither *HGF* nor *IL6* gene expression levels were different between the CBZ-treated livers and vehicle-treated livers following PHx (Supplementary Fig. 4A and B). By contrast, in the *in vitro* study, primary hepatocytes presented sustained phosphorylation of Akt (Ser473) with transient and moderate activation of mTOR in response to the administration of CBZ (Supplementary Fig. 5). These findings support the idea that CBZ may directly activate intracellular signalling pathways in hepatocytes contributing to enhanced liver regeneration. Meanwhile, in this *in vitro* setting, primary hepatocytes did not show a proliferative response to CBZ administration (Supplementary Fig. 6). This may be because hepatocytes require additional priming stimulus to start proliferation *in vitro*, same as our *in vivo* finding that CBZ administration did not start liver regeneration in the sham-operated mice (Fig. 1E and F, and Supplementary Fig. 1). We cannot exclude the possibility that CBZ does not primarily target hepatocytes, but affects other cell types in the liver to promote liver regeneration. Actual targets of CBZ in the liver will be determined in future studies.

In rodents, 70% hepatectomy is well tolerated, but beyond 70%, resection is accompanied by higher mortality due to acute liver failure despite the inherent ability of the liver to recover to full size. This suggests that insufficient functional compensation of the remnant liver fails to maintain homeostasis in the animal [16,27]. In clinical settings, extended liver resection is reportedly associated with severe hepatic dysfunction, leading to a significant increase in postoperative mortality [33,34]. In this context, the promotion of the recovery of impaired liver function is critically important for any therapeutic drug potentially used to aid in liver regeneration. In the present study, CBZ treatment significantly improved the survival rate of the mice that underwent lethal 85% massive hepatectomy. This result elucidates the therapeutic potential of CBZ to prevent postoperative liver failure after major hepatectomy or living donor liver transplantation with extended criteria.

When considering the therapeutic application of this study, it is important to apply clinically relevant doses of CBZ to obtain relevant physiological serum levels of CBZ (4-12 μg/ml) [35]. In the present study, 2 h after oral administration of 250 mg/kg of CBZ, its serum level reached 22.9 μg/ml (Supplementary Fig. 7A) and was relatively higher than the therapeutic range in humans. It is known that repeated administration of CBZ shortens its half-life, and therefore consecutive administration is required to acquire steady state levels [19]. Thus, we evaluated CBZ serum levels after repeated administration at 250 mg/kg for 3 consecutive days. This administration method acquires physiological levels of CBZ (4.8 μg/ml) (Supplementary Fig. 7B), and importantly, the favorable effect on liver regeneration was retained in the subsequently performed 70% PHx (Supplementary Fig. 2A and B). This result may support the potential therapeutic use of CBZ. We also studied the influence of hepatectomy on serum levels of CBZ because it reduces the total amount of metabolizing cells in the liver. Serum levels of CBZ were not different between the hepatectomized mice and the sham operated mice 3 h after the surgery (Supplementary Fig. 7C), suggesting that CBZ treatment may be applicable after liver resection.

In conclusion, we demonstrated that CBZ promoted hepatocyte proliferation via the mTOR signalling pathway, resulting in early liver regeneration in mice. We also demonstrated the therapeutic implications of this drug in an 85% massive hepatectomy model. Despite a large number of basic studies searching for novel therapeutic agents to enhance liver regeneration, few options are currently available for clinical use [6,7]. Our study suggests the possibility that CBZ may enhance liver regeneration in a clinical setting, leading to a reduction in postoperative liver failure and improving survival.

Conflict of interest

The authors who have taken part in this study declared that they do not have anything to disclose regarding funding or conflict of interest with respect to this manuscript.

Supplementary data

Supplementary data associated with this article can be found, in the online version, at http://dx.doi.org/10.1016/j.jhep.2013.07.018.

References

[1] Fausto N. Liver regeneration. J Hepatol 2000;32:19–31.
[2] Karp SJ. Clinical implications of advances in the basic science of liver repair and regeneration. Am J Transplant 2009;9:1973–1980.
[3] Michalopoùlos GK, DeFrances MC. Liver regeneration. Science 1997;276:60–66.
[4] Shirabe K, Shimada M, Gion T, Hasegawa H, Takenaka K, Utsunomiya T, et al. Postoperative liver failure after major hepatic resection for hepatocellular carcinoma in the modern era with special reference to remnant liver volume. J Am Coll Surg 1999;188:304–309.
[5] Balzan S, Belghiti J, Farges O, Ogata S, Sauvanet A, Delefosse D, et al. The "50–50 criteria" on postoperative day 5: an accurate predictor of liver failure and death after hepatectomy. Ann Surg 2005;242:824–828, [discussion 828–829].
[6] Ishiki Y, Ohnishi H, Muto Y, Matsumoto K, Nakamura T. Direct evidence that *hepatocyte growth factor is a hepatotrophic factor for liver regeneration and* has a potent antihepatitis effect in vivo. Hepatology 1992;16:1227–1235.
[7] Zimmers TA, McKillop IH, Pierce RH, Yoo JY, Koniaris LG. Massive liver growth in mice induced by systemic interleukin 6 administration. Hepatology 2003;38:326–334.
[8] Post RM, Denicoff KD, Frye MA, Dunn RT, Leverich GS, Osuch E, et al. A history of the use of anticonvulsants as mood stabilizers in the last two decades of the 20th century. Neuropsychobiology 1998;38:152–166.
[9] Stahl SM. Anticonvulsants as mood stabilizers and adjuncts to antipsychotics: valproate, lamotrigine, carbamazepine, and oxcarbazepine and actions at voltage-gated sodium channels. J Clin Psychiatry 2004;65:738–739.
[10] Chalecka-Franaszek E, Chuang DM. Lithium activates the serine/threonine kinase Akt-1 and suppresses glutamate-induced inhibition of Akt-1 activity in neurons. Proc Natl Acad Sci U S A 1999;96:8745–8750.
[11] Coyle JT, Duman RS. Finding the intracellular signaling pathways affected by mood disorder treatments. Neuron 2003;38:157–160.
[12] Duman RS, Malberg J, Nakagawa S, D'Sa C. Neuronal plasticity and survival in mood disorders. Biol Psychiatry 2000;48:732–739.
[13] Mai L, Jope RS, Li X. BDNF-mediated signal transduction is modulated by GSK3beta and mood stabilizing agents. J Neurochem 2002;82:75–83.
[14] Hidvegi T, Ewing M, Hale P, Dippold C, Beckett C, Kemp C, et al. An autophagy-enhancing drug promotes degradation of mutant alpha1-antitrypsin Z and reduces hepatic fibrosis. *Science 2010;329:229–232.*
[15] Mitchell C, Willenbring H. A reproducible and well-tolerated method for 2/3 partial hepatectomy in mice. Nat Protoc 2008;3:1167–1170.
[16] Cataldegirmen G, Zeng S, Feirt N, Ippagunta N, Dun H, Qu W, et al. RAGE limits regeneration after massive liver injury by coordinated suppression of TNF-alpha and NF-kappaB. J Exp Med 2005;201:473–484.
[17] Espeillac C, Mitchell C, Celton-Morizur S, Chauvin C, Koka V, Gillet C, et al. S6 kinase 1 is required for rapamycin-sensitive liver proliferation after mouse hepatectomy. J Clin Invest 2011;121:2821–2832.
[18] Kodama T, Takehara T, Hikita H, Shimizu S, Shigekawa M, Tsunematsu H, et al. Increases in p53 expression induce CTGF synthesis by mouse and human hepatocytes and result in liver fibrosis in mice. J Clin Invest 2011;121:3343–3356.
[19] Eichelbaum M, Ekbom K, Bertilsson L, Ringberger VA, Rane A. Plasma kinetics of carbamazepine and its epoxide metabolite in man after single and multiple doses. Eur J Clin Pharmacol 1975;8:337–341.
[20] Yamada Y, Fausto N. Deficient liver regeneration after carbon tetrachloride injury in mice lacking type 1 but not type 2 tumor necrosis factor receptor. Am J Pathol 1998;152:1577–1589.
[21] Sun R, Gao B. Negative regulation of liver regeneration by innate immunity (natural killer cells/interferon-gamma). Gastroenterology 2004;127:1525–1539.
[22] Borowiak M, Garratt AN, Wustefeld T, Strehle M, Trautwein C, Birchmeier C. *Met provides essential signals for liver regeneration.* Proc Natl Acad Sci U S A 2004;101:10608–10613.
[23] Coutant A, Rescan C, Gilot D, Loyer P, Guguen-Guillouzo C, Baffet G. PI3K-FRAP/mTOR pathway is critical for hepatocyte proliferation whereas MEK/ERK supports both proliferation and survival. Hepatology 2002;36:1079–1088.
[24] Fausto N, Campbell JS, Riehle KJ. Liver regeneration. Hepatology 2006;43:S45–S53.
[25] Talarmin H, Rescan C, Cariou S, Glaise D, Zanninelli G, Bilodeau M, et al. The mitogen-activated protein kinase kinase/extracellular signal-regulated kinase cascade activation is a key signalling pathway involved in the regulation of G(1) phase progression in proliferating hepatocytes. Mol Cell Biol 1999;19:6003–6011.
[26] Schwabe RF, Bradham CA, Uehara T, Hatano È, Bennett BL, Schoonhoven R, et al. C-Jun-N-terminal kinase drives cyclin D1 expression and proliferation during liver regeneration. Hepatology 2003;37:824–832.
[27] Panis Y, McMullan DM, Emond JC. Progressive necrosis after hepatectomy and the pathophysiology of liver failure after massive resection. Surgery 1997;121:142–149.
[28] Decker T, Hipp S, Ringshausen I, Bogner C, Oelsner M, Schneller F, et al. Rapamycin-induced G1 arrest in cycling B-CLL cells is associated with reduced expression of cyclin D3, cyclin E, cyclin A, and survivin. Blood 2003;101:278–285.
[29] Dai G, He L, Bu P, Wan YJ. Pregnane X receptor is essential for normal progression of liver regeneration. Hepatology 2008;47:1277–1287.
[30] Borude P, Edwards G, Walesky C, Li F, Ma X, Kong B, et al. Hepatocyte-specific deletion of farnesoid X receptor delays but does not inhibit liver regeneration after partial hepatectomy in mice. Hepatology 2012;56:2344–2352.
[31] Zhang L, Wang YD, Chen WD, Wang X, Lou G, Liu N, et al. Promotion of liver regeneration/repair by farnesoid X receptor in both liver and intestine in mice. Hepatology 2012;56:2336–2343.
[32] Selzner N, Selzner M, Odermatt B, Tian Y, Van Rooijen N, Clavien PA. ICAM-1 triggers liver regeneration through leukocyte recruitment and Kupffer cell-dependent release of TNF-alpha/IL6 in mice. Gastroenterology 2003;124:692–700.
[33] Schindl MJ, Redhead DN, Fearon KC, Garden OJ, Wigmore SJ. The value of residual liver volume as a predictor of hepatic dysfunction and infection after major liver resection. Gut 2005;54:289–296.
[34] Jarnagin WR, Gonen M, Fong Y, DeMatteo RP, Ben-Porat L, Little S, et al. Improvement in perioperative outcome after hepatic resection: analysis of 1803 consecutive cases over the past decade. Ann Surg 2002;236:397–406, [discussion 406–397].
[35] St Louis EK, Louis EK. Minimizing AED adverse effects: improving quality of life in the interictal state in epilepsy care. Curr Neuropharmacol 2009;7:106–114.

Biochemical and Biophysical Research Communications 437 (2013) 127–133

Contents lists available at SciVerse ScienceDirect

Biochemical and Biophysical Research Communications

journal homepage: www.elsevier.com/locate/ybbrc

Valine, the branched-chain amino acid, suppresses hepatitis C virus RNA replication but promotes infectious particle formation

Hisashi Ishida [a], Takanobu Kato [b], Kenji Takehana [c], Tomohide Tatsumi [a], Atsushi Hosui [a], Takatoshi Nawa [a], Takahiro Kodama [a], Satoshi Shimizu [a], Hayato Hikita [a], Naoki Hiramatsu [a], Tatsuya Kanto [a], Norio Hayashi [d], Tetsuo Takehara [a,*]

[a] Department of Gastroenterology and Hepatology, Osaka University Graduate School of Medicine, 2-2, Yamadaoka, Suita, Osaka, Japan
[b] Department of Virology II, National Institute of Infectious Diseases, Tokyo, Japan
[c] Exploratory Research Laboratories, Research Center, Ajinomoto Pharmaceuticals, Co, Ltd., Kanagawa, Japan
[d] Kansai Rosai Hospital, Amagasaki, Hyogo, Japan

ARTICLE INFO

Article history:
Received 3 June 2013
Available online 24 June 2013

Keywords:
Hepatitis C virus
Branched-chain amino acid
IRES activity
Infectious virus production
Mammalian target of rapamycin
JAK/STAT pathway

ABSTRACT

Background & aims: Concentrations of the branched-chain amino acid (BCAA) in the serum of patients with liver cirrhosis correlate with their liver function. Oral administration of BCAA can ameliorate hypoalbuminemia and hepatic encephalopathy. In this study, we aim to clarify the role of BCAA in regulating the replication of the hepatitis C virus (HCV).
Methods: HCV sub-genomic replicon cells, genome-length replicon cells, and cells infected with cell culture-infectious HCV (HCVcc) were cultured in media supplemented with various concentrations of BCAA, followed by evaluation of the replicon or HCV abundance.
Results: BCAA was capable of suppressing the HCV replicon in a dose-dependent manner and the effect was independent of the mTOR pathway. Of the three BCAAs, valine was identified as being responsible for suppressing the HCV replicon. Surprisingly, an abundance of HJ3-5(YH/QL), an HCVcc, in Huh7 cells was augmented by BCAA supplementation. In contrast, BCAA suppressed an abundance of HJ3-5(wild), an HCVcc that cannot assemble virus particle in Huh7 cells. Internal ribosome entry site of HCV was shown to be a target of BCAA. Single-cycle virus production assays using Huh7-25 cells, which lacked CD81 expression, revealed that BCAA, especially valine, promoted infectious virus particle formation with minimal effect on virus secretion. Thus, BCAA was found to have two opposing effects on HCV production: suppression of the HCV genome RNA replication and promotion of infectious virus formation.
Conclusions: BCAA accelerates HCV production through promotion of infectious virus formation in infected cells despite its suppressive effect on HCV genome replication.

1. Introduction

Persistent infection of hepatitis C virus (HCV) causes progressive liver disease in humans. Chronic inflammation in the liver leads to the accumulation of fibrosis and an eventual progression to liver cirrhosis. In patients with decompensated liver cirrhosis, a change in plasma amino acid composition is frequently observed. In particular, the ratio of branched-chain amino acid (BCAA) to aromatic amino acid (AAA), known as Fischer's ratio, decreases as the liver function deteriorates [1]. In such cirrhotic patients, hypoalbuminemia occurs, and it has been shown that oral administration of BCAA can ameliorate hypoalbuminemia and hepatic encephalopathy.

Three amino acids valine, leucine, and isoleucine are BCAAs, which are considered to be essential for protein anabolism. In addition to the role of acting as nutrient substrates, recent studies have demonstrated that BCAA also serve as physiologically active substances. BCAA have been shown to have pharmacological effects, such as induction of protein synthesis [2] and glucose metabolism [3]. In rat primary hepatocytes, albumin synthesis is significantly increased by BCAA administration, which is dependent on activation of the mammalian target of rapamycin (mTOR), mainly induced by leucine [4].

HCV replication is controlled by intracellular signaling pathways. In addition to the interferon (IFN)-induced JAK/STAT pathway, which activates interferon-stimulated genes, leading to strong anti-viral activity, activation of ERK [5], PI3 kinase/Akt [6,7], smad [8], PKC [9], and p38 [10], have been shown to be capable of regulating HCV replication. mTOR, one of the downstream molecules of Akt, phosphorylates the two substrates p70 S6 kinase and eukaryotic translation initiation factor 4E binding protein 1

* Corresponding author. Address: Department of Gastroenterology and Hepatology, Osaka University Graduate School of Medicine, 2-2, Yamadaoka, Suita, Osaka 565-0871, Japan. Fax: +81 6 6879 3629.
E-mail address: takehara@gh.med.osaka-u.ac.jp (T. Takehara).

0006-291X/$ - see front matter © 2013 Elsevier Inc. All rights reserved.
http://dx.doi.org/10.1016/j.bbrc.2013.06.051

(4EBP1). p70 S6 kinase phosphorylates ribosomal S6 protein, resulting in an increase of the protein synthesis complex. Phosphorylated 4EBP1 results in its dissociation from the eukaryotic translation initiation factor 4E (eIF4E), which consequently enables eIF4E to regulate the translation initiation. Thus, together, p70 S6 kinase and 4EBP1 are responsible for the mTOR-dependent regulation of cellular translation. Moreover, both have been demonstrated to be involved in the regulation of HCV replication [6].

The finding that BCAA, per se, can activate signaling pathways suggests that they may affect HCV replication, presumably via the activation of the mTOR pathway. However, to date, no detailed investigation has been reported. Therefore, we attempt to clarify whether BCAA have a role in regulating HCV replication by using the HCV replicon system and cell culture of infectious-HCV (HCVcc). The present study reveals that although BCAA, especially valine, suppresses HCV genome replication, they eventually promote total HCV production by accelerating viral formation.

2. Methods

2.1. Cells

The hepatoma-derived cell line Huh7 and its derivatives, Huh7.5 and Huh7-25 [11], were maintained in DMEM supplemented with 10% FCS. The HCV subgenomic replicon cell line Huh-RepSI [10], and the HCV genome-length replicon cell line 2–3 [12], both harboring the HCV-N strain (genotype 1b), were previously described. The molar ratio of the BCAA mixture was adjusted to Leu:Ile:Val = 2.0:1.0:1.2 according to data from previous studies [13]. For assays to examine the role of BCAA, cells were cultured in BCAA-deficient DMEM with 10% FCS supplemented with BCAA mixtures of various concentrations (0–2 mM).

2.2. Cell culture-infectious HCV

JFH-1 is a cell culture-infectious virus of genotype 2a as previously described [14]. HJ3-5(YH/QL) is a chimeric cell culture-infectious virus with a genome consisting of the core to NS2 sequence of genotype 1a (H77) virus placed within the background of the genotype 2a JFH-1 virus. This virus contained compensatory mutations in E1 (Y361H) and NS3 (Q1251L) [15]. These two mutations rendered the chimeric RNA highly infectious.

2.3. In Vitro transcription and transfection of synthetic RNA

Plasmid DNAs encoding HJ3-5(wild) and HJ3-5(YH/QL), a wild-type chimeric virus and a chimeric virus carrying two mutations, respectively, were linearized by *Xba*I prior to transcription. RNA was synthesized with the T7 RiboMAX Express Large Scale RNA Production System (Promega, Madison, WI, USA) following the

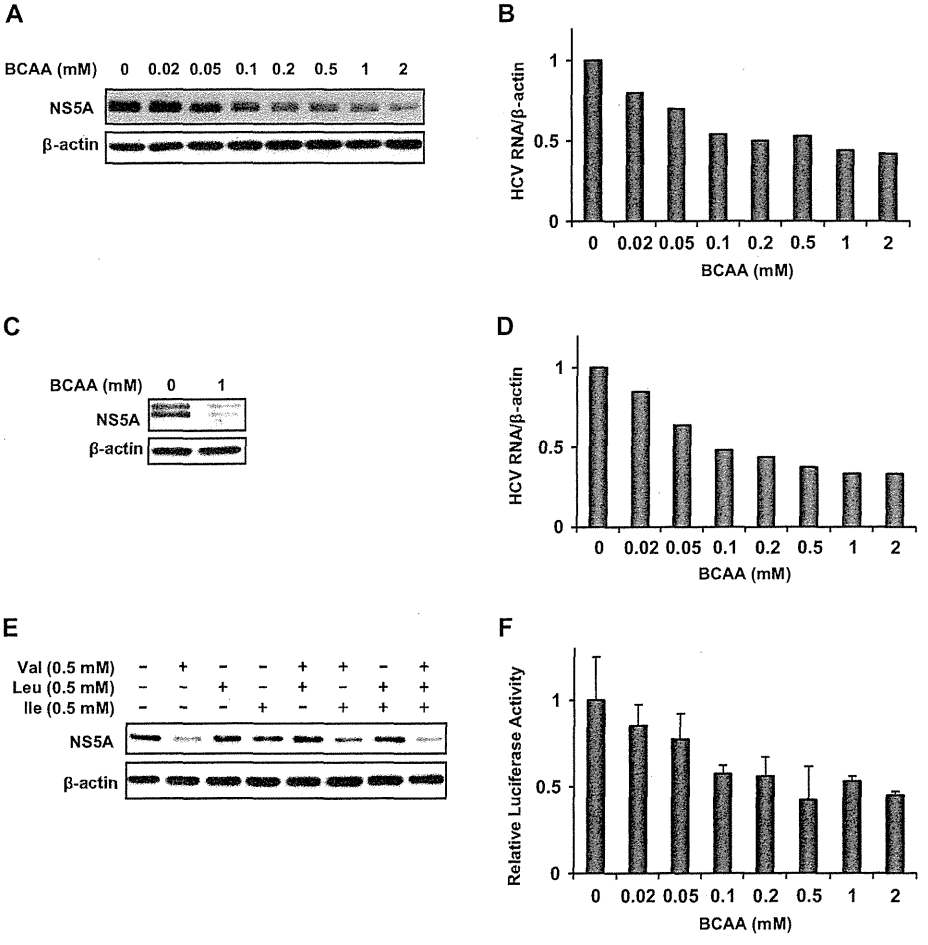

Fig. 1. BCAA limits the abundance of HCV replicon in HCV replicon cells. (A–D). Huh-RepSI (A and B) and 2-3 (C and D) cells were cultured in media for 2 days, with BCAA supplemented at concentrations of 0–2 mM. Total protein or total RNA was recovered and assayed for immunoblot (A and C) or real-time RT-PCR (B and D), respectively. (E) Three BCAAs (0.5 mM each) were added to BCAA-free culture medium of Huh-RepSI. After incubation for 2 days, immunoblot analysis of NS5A and beta-actin were performed. (F) Huh-RepSI cells were transfected with pRLHL, cultured in media with various BCAA concentrations between 0 and 2 mM. After incubation for 2 days, a dual luciferase assay was performed. The ratio of firefly luciferase activity to renilla luciferase activity was then calculated.

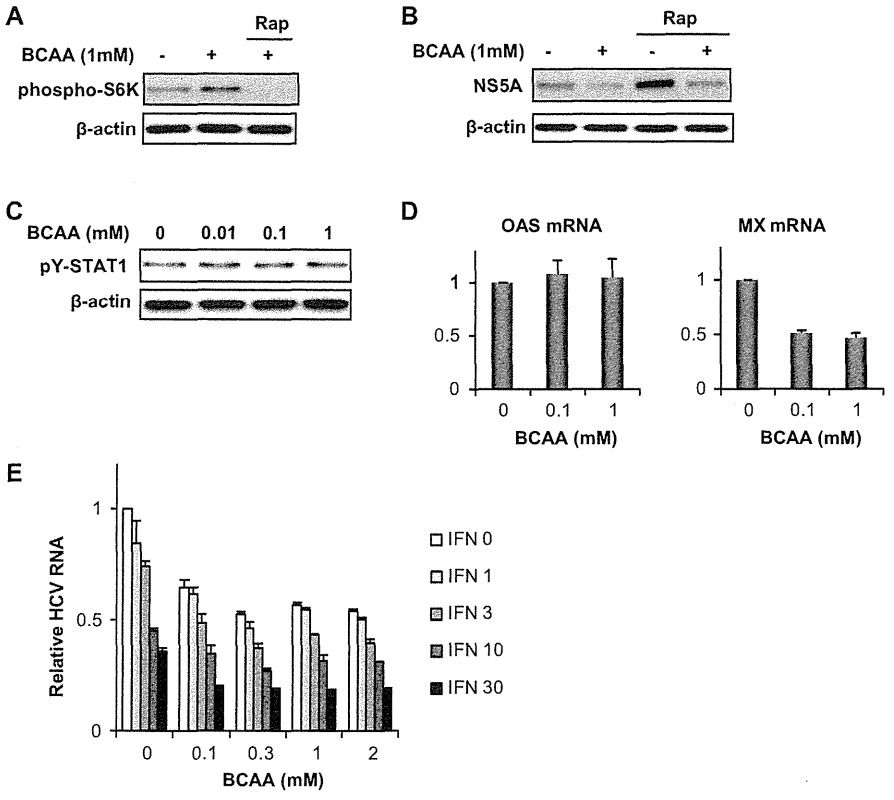

Fig. 2. BCAA-induced suppression of HCV replicon is independent of mTOR or JAK/STAT signaling. (A) Immunoblot of phosphorylated p70 S6 kinase and beta-actin in Huh-RepSI cells cultured in a medium with or without BCAA (1 mM). Rapamycin was added at 100 nM to the BCAA-containing medium. (B) Immunoblot analysis of NS5A and beta-actin in Huh-RepSI cells cultured in a medium with 1 mM BCAA or rapamycin (100 nM). (C) Huh-RepSI cells were incubated in media with various BCAA concentrations (0, 0.01, 0.1, 1 mM), and then, immunoblot analyses of phosphorylated STAT1 (Tyr701) and beta-actin were performed. (D) Huh-RepSI cells were incubated in media with various BCAA concentrations (0, 0.1, 1 mM), and then, a real-time RT-PCR analysis, for expression of OAS and MX, was performed. (E) Huh-RepSI cells were incubated in culture media with various BCAA concentrations (0–2 mM) and IFN-α (0–30 U/ml). HCV RNA abundance was normalized with beta-actin allowing the relative HCV RNA levels to be calculated, setting the HCV RNA level of 0 U/ml IFN-α and 0 mM BCAA as 1. Rap: rapamycin.

manufacturer's suggested protocol. For electroporation, Huh7 cells were washed twice with ice cold phosphate-buffered saline (PBS) and resuspended at a concentration of 10^7 cells/ml in PBS. Subsequently, 10 μg of RNA was mixed with 500 μl of the cell suspension in a cuvette, with a gap width of 0.2 cm (GenePulser II System; Bio-Rad, Hercules, CA, USA). The mixture was immediately subjected to two pulses of current with the intensities of 1.2 kV, 25 μF, and maximum resistance. Following a 10-min incubation at room temperature, the cells were transferred into growth medium.

2.4. Titration of HCV infectivity

Huh-7.5.1 cells were seeded in 96-well plates at a density of 1×10^4 cells per well 24 h prior to culture media inoculation of the HCV infected cells. Three days after infection, HCV-positive cells were detected with mouse monoclonal antibody that recognized core proteins stained with an Alexa Fluor 488 anti-mouse secondary antibody (Invitrogen, Carlsbad, CA, USA). The infectivity titer was expressed as focus-forming units per mL of supernatant (ffu/mL), expressing the mean number of HCV core-positive foci. The intracellular infectivity and specific intracellular infectivity titer were determined as described previously [16].

3. Results

3.1. BCAA suppresses the amount of HCV replicon

To investigate the role of BCAA in HCV replication, we first examined the effect of BCAA on the HCV replicon. An HCV subgenomic replicon cell line, Huh-RepSI, was incubated in culture medium that contained various concentrations of BCAA (0–2 mM) for 2 days. HCV replicon RNA, as well as the amount of protein, was suppressed by adding BCAA in a dose-dependent manner (Fig. 1A and B). To confirm the effect of BCAA, another replicon cell line, 2–3, carrying a genome-length HCV replicon, was used. In this experiment, suppression of the replicon by BCAA was observed, which is in agreement with the Huh-RepSI assay (Fig. 1C and D). This activity suggested that BCAA possessed the ability to suppress HCV replication.

Three BCAAs exist: valine, leucine, and isoleucine. As previously demonstrated, leucine contains the biological activity to activate mTOR. In addition, we showed that mTOR, which is activated by PI3 kinase/Akt, was able to suppress HCV replication [6]. Therefore, it is possible that the BCAA-mediated suppression of HCV replication was due to leucine. To test this hypothesis, the three amino acids were added independently to BCAA-deficient medium while monitoring the HCV replication level. Unexpectedly, the result refuted the hypothesis (Fig. 1E). Compared to the cells cultured in BCAA-deficient medium, supplementation with only valine efficiently suppressed the HCV replicon, whereas leucine did not; instead, it caused a slight increase. This result showed that BCAA, especially valine, but not leucine, have a suppressive effect on HCV replication.

3.2. BCAA suppresses HCV IRES activity

HCV replication can be controlled by HCV specific translation regulated by IRES, the 5′ UTR region of HCV. Therefore, we next

investigated the effect of BCAA on HCV IRES activity. To do this, we utilized a dicistronic vector, pRLHL, which consists of firefly luciferase driven by HCV IRES and renilla luciferase, translated in a cap-dependent manner (Sup. Fig. 1). Relative HCV IRES activity was evaluated using the ratio of IRES-specific luciferase activity to the cap-dependent luciferase activity. As shown in Fig. 1F, HCV IRES activity was suppressed by BCAA in a dose-dependent manner, which is similar to the result of the replicon abundance (Fig. 1A and B). Thus, the BCAA-mediated suppression of HCV replication is likely due to the inhibition of HCV IRES activity.

3.3. BCAA-mediated suppression of HCV replicon is independent of the mTOR and JAK/STAT pathways

Previous reports have demonstrated that BCAA is capable of activating mTOR [4], and we have reported that mTOR suppresses HCV replication [6]. Therefore, we examined the contribution of mTOR activation on BCAA-mediated suppression of the HCV replicon. Administration of BCAA efficiently phosphorylated p70 S6 kinase, whereas rapamycin completely inhibited its phosphorylation (Fig. 2A). Despite rapamycin enhancing the amount of HCV replicon, BCAA could efficiently suppress it, even in rapamycin-containing medium (Fig. 2B), suggesting that the suppression of the HCV replicon by BCAA is independent of mTOR activation.

The IFN-JAK/STAT signal is known to be an anti-virus pathway, induced under the condition of virus infection. HCV replication is efficiently inhibited by interferon. Therefore, we examined whether BCAA could modify the IFN signal. First, we performed an immunoblot analysis and evaluated the status of STAT1 activation, in the presence or absence of BCAA. However, the phosphorylated STAT1 level was not altered by BCAA in Huh-RepSI cells, and ISG induction was not observed; instead, the expression level of Mx was suppressed by BCAA (Fig. 2C and D). A previous study showed that rapamycin diminished the suppressive effect of IFN-α toward HCV replication via the suppression of ISG induction [17]. Subsequently, we examined the HCV replicon abundance in cells that were cultured in media with various concentrations of BCAA and IFN-α stimuli. Even with the depletion of BCAA, IFN-α efficiently and dose-dependently suppressed HCV replicon abundance. However, IFN-α-induced anti-HCV activity was not augmented by BCAA supplementation (for example, the replicon RNA level decreased to approximately 30% in both BCAA-depleted medium and 2 mM BCAA-supplemented medium) (Fig. 2E). Consequently, BCAA did not influence JAK/STAT activation, and therefore, the suppression of HCV replicon by BCAA may have been independent of the IFN-α-induced signaling pathway.

3.4. BCAA enhances HCVcc production

Next, we examined the impact of BCAA on HCVcc, a system retaining the entire HCV life cycle in a cultured cell. Here, we used HJ3-5(YH/QL), a chimeric HCV of genotype 1a (H77) and 2a (JFH-1). Surprisingly, the results of HJ3-5(YH/QL) were opposite to that of the HCV replicon: HCV abundance was upregulated in a BCAA dose-dependent manner (Fig. 3A). The HCV replicon contains NS3 to NS5B proteins, which are required for HCV RNA genome replication, but not core, E1 and E2 proteins, which are structural proteins required for viral particle formation. The discrepancy in the results between HCV replicon cells and HCVcc-infected cells might be due to differences in virus particle production.

To investigate this discrepancy, we used the wild-type HJ3-5, designated as HJ3-5(wild). As described in the Methods section, HJ3-5(YH/QL) or the HCVcc used in this study, carries two amino acid substitutions at amino acid 361 and amino acid 1251, within E1 and NS3, respectively. These two mutations render the chimeric RNA highly infectious [15]. However, without these mutations, virus particle assembly and consequent virion release from the cells to the medium would not occur. This process is thought to be due to impaired association of the HCV proteins originating from different genotypes, whereas there is no apparent change in the HCV RNA replication level in the cells [15].

We introduced the *in vitro* transcribed genome RNA of HJ3-5(wild) or HJ3-5(YH/QL) into Huh7 cells with electroporation, and then, we examined the effect of BCAA on the cell line. Normally, synthesized HCV RNA introduced into cells executes replication by utilizing HCV proteins encoded in the genome and host factors, resulting in a robust increase that is detectable after 2–3 days. BCAA decreased the abundance of HJ3-5(wild), which was similar to their effect on the HCV replicon (Fig. 3B and C). Thus, HJ3-5(wild), a virus that is defective in virus particle formation, revealed the opposite reaction to BCAA compared to the virus HJ3-5(YH/QL), a virus that is competent in virus particle formation. Together, these findings revealed that although BCAA had the ability to suppress the HCV genome replication, they promoted viral production by enhancing other steps, which included virus assembly, virus particle release and cell re-infection.

3.5. BCAA promotes infectious HCV particle formation, not virus secretion

To further assess the BCAA intracellular mechanisms that influence the HCV life cycle, we adopted a single-cycle virus production assay [18]. We used Huh7-25 cells due to the lack of surface expression of one of the cellular HCV receptors, CD81, thus being non-permissive to HCV infection. Because HCV genome replication or virus production is intact in Huh7-25, we can evaluate viral replication and secretion without the influence of re-infection.

First, we studied the replication levels of the infectious virus, JFH-1, in Huh7-25 cells. The full length of the JFH-1 genome RNA

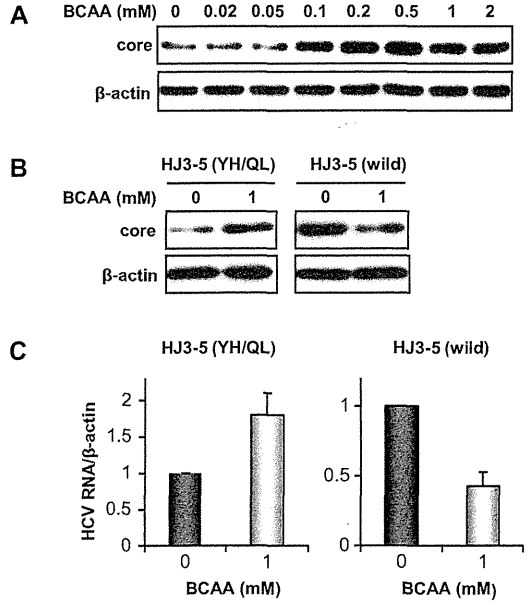

Fig. 3. HCVcc abundance was increased by BCAA. (A) HCVcc-infected Huh7 cells were cultured in media with various BCAA concentrations (0–2 mM). After incubation for 2 days, and an immunoblot analysis of core and beta-actin was performed. (B and C) Synthesized HCV genome RNA of HJ3-5 (YH/QL) or HJ3-5 (wild) was transfected into Huh7 cells via electroporation. After incubation for 24 h, cells were split into 6-well plates and incubated for 2 days in a culture medium with or without 1 mM BCAA. After the cells were harvested, immunoblot analysis of core and beta-actin (B) and real-time RT-PCR analysis (C) were performed.

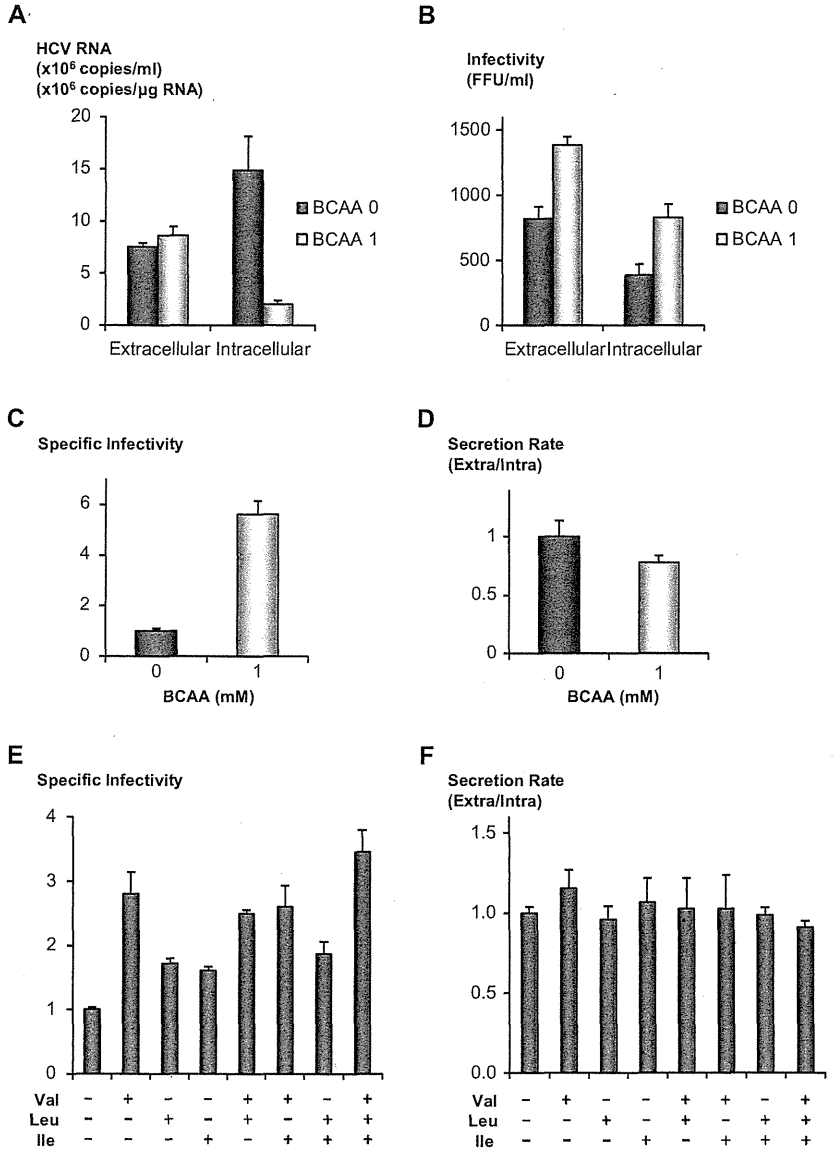

Fig. 4. Single-cycle virus production assay indicates a promoting effect of BCAA on virus formation. (A) Huh7-25 cells were transfected with *in vitro*-transcribed RNA of JFH-1, incubated in media with or without BCAA, followed by the RNA levels in the media or in the cells being calculated using the real-time quantitative RT-PCR method. (B) Infectivities in the media or in the cell lysates were measured. (C) Specific infectivities were calculated by dividing the infectivities by the HCV RNA amounts. (D) Secretion rates were calculated by dividing extracellular infectivities by intracellular infectivities. The data were presented as ratios defining the value of BCAA at 0 mM as 1. (E and F) Specific infectivities and secretion rates in the presence of valine (0.5 mM), leucine (0.5 mM), or isoleucine (0.5 mM). The data were presented as ratios defining the value with no BCAA as 1.

was translated *in vitro* and transfected into the Huh7-25 cells. The cells were cultured in media, with or without 1 mM of BCAA, with the RNA levels being monitored using quantitative RT-PCR. As observed in the experiment of replicon cells or virus particle formation-deficient viruses, the intracellular RNA level of HCV was suppressed by the presence of BCAA (Fig. 4A). However, the levels of extracellular HCV RNA were similar. Despite the suppression of intracellular HCV RNA levels by BCAA-containing medium, the infectivity titer of the intracellular virus in the cells treated with 1 mM BCAA was significantly higher than that of the cells with 0 mM BCAA (Fig. 4B). Extracellular infectivity titers were similar to those of intracellular infectivity. The specific infectivity of intracellular virus was calculated by dividing the infectivity titer by the HCV RNA level and this revealed that cultivation of the cells in a medium of 1 mM BCAA resulted in a 5.6-fold higher specific virus infectivity than that of 0 mM BCAA (Fig. 4C). Next, we measured virus secretion rates by dividing extracellular infectivity titers by intracellular infectivity titers. There was a minimal difference between infectious virus particle secretions (Fig. 4D). Thus, these results indicated that the infectious virion production was promoted in the BCAA-supplemented medium, although the virus RNA replication was suppressed.

In the study using replicon cells, valine was shown amino acid responsible for regulating HCV RNA replication (Fig. 1E). Finally, we assessed the effect of individual BCAA on virus production. HCV infected cells were cultured in media containing each amino acid at 0.5 mM or a combination of them and subsequently specific infectivity and secretion rate were examined (Fig. 4E and F). Among the three BCAAs, valine promoted infectious virus production most effectively, while leucine and isoleucine promoted infectious virus production modestly. Secretion rates did not show a significant difference.